Kinematic and petrologic analysis of Alpine structures in the Axial Zone of the Pyrenees, Spain

Kuiper, M.E.

Department of Earth Sciences
Utrecht University, Utrecht, The Netherlands

MSc-thesis under supervision of Dr. E. Willingshofer & Prof. Dr. M.R. Drury

Abstract

In the Axial-Zone of the Pyrenees, in the Pallars Sobirà, Northern Pallars Jussà and Alta Ribargorça regions, a field research has been conducted in order to understand the difference in kinematics between the Variscan and Alpine orogenies, respectively. Structural mapping has been complemented with microstructural and petrologic investigations of Paleozoic rocks from the Axial Zone in order to constrain pressure and temperature conditions during deformation. Furthermore, measurements have been taken of faults and foliations in the studied area. This data has been plotted in stereographic projections to compare the two major deformation phases which have affected the Axial Zone of the Pyrenees. From this study it can be concluded that there is a slight difference in the kinematics of the Variscan and Alpine orogeny. There are three deformation event recognized. An old deformation phase resulting in a penetrative S1 foliation which has been crenulated by a younger C^1 structure. These structures have been deformed by the youngest deformation phase reactivating faults and creating an antiformal stack in the central Pyrenees. Small difference in the orientation of the shortening direction between the two orogenies to be found in the studied area. The Variscan orogeny shows general shortening in the NNE-SSW direction, whereas the Alpine orogeny is more N-S. From the petrologic analysis of the thin sections, it can be concluded from analyzing the twinning structures in the calcite minerals, that the pressure and temperature conditions during the Variscan orogeny for the currently exposed rocks near Llavorsi lie around 107 MPa and 300°C.

Keywords: Tec-Lab, Llavorsi, Axial Zone, Pyrenees, kinematic analysis, petrologic analysis, Paleozoic meta-sediments, Variscan orogeny, Alpine orogeny, Maladeta

Table of content

1. Introduction

On the border between France and Spain lie the Pyrenees, a mountain range caused by the collision between the Eurasian plate and the Iberian plate. The orogen consists of an asymmetrical double vergent tectonic wedge and is divided into several structural zones (see figure 1) (*Sibuet, 2004*). These zones are the Northern Foreland, North Pyrenean Zone, Axial Zone, South Pyrenean Units, and the Southern foreland (*Choukroune, 1992*). The Northern and Southern foreland together with the North Pyrenean Zone and South Pyrenean Units consist of Mesozoic sediments. The Axial zone consists of Paleozoic and Phanerozoic lithologies. This zone contains structures and rocks affected by the Variscan orogeny, which occurred between ca. 420 and 290 Ma (*Matte, 2001*). These deformed rocks encountered a second deformation phase during the Alpine orogeny (100 – 0 Ma) in which the current Pyrenees were formed. In the field of structural analysis, there has been a lot of work in the Pyrenean mountains. Based on the deep reflection seismic profile, ECORS, and related geological investigations major advances on the understanding of the Alpine structure of the Pyrenees have been made (*Choukroune, 1989, Zwart, 1986*).

Although there is overall agreement on the structure of the Pyrenees, the kinematic evolution of the mountain belt and in particular of the internal zone is not studied very well. The rocks in the Axial Zone of the Pyrenees are Paleozoic meta-sediments with multiple massifs that intruded these rocks during the Variscan orogeny (*Evans, 1998*). The structures in these rocks are primarily of Variscan age. During the Variscan phase, metamorphism of the Paleozoic sediments reached greenschist facies conditions (*Zwart,*

1986). The structures in the Axial Zone we find today, have been affected by an Alpine overprint and it is often not clear as-to-whether lower greenschist facies shear zones are related to the Alpine or the Variscan phase of deformation. Moreover, their significance for the exhumation of rocks is largely unknown and forms the centerpiece of this study.

2. Architecture of the Pyrenees

The Pyrenees are comprised of several structural zones (*Sibuet, 2004*), notably the Northern Foreland, Northern Pyrenean Zone, Axial Zone, South Pyrenean Units and the Southern Foreland. The structure of these units is studied through the ECORS deep reflection seismic project (*Choukroune, 1990*), which forms the backbone of the cross-section of the Pyrenees, shown in figure 1. The Northern Foreland and North Pyrenean zone, Southern Pyrenean Units and Southern Foreland represent the foreland basins of the Pyrenees after the Variscan Orogeny. These basins are comprised of Mesozoic sediments which now form the thrustbelts we see today (e.g. Sierra del Montsec, Sierras Marginales) with Tertiary sediments on either side in foreland basins. The thrustbelts have mainly a top to the south transport direction and are oriented parallel to the overall East-West strike of the Pyrenees.

The first order structures comprising the Axial Zone are a large antiformal stack including the whole axial zone. This antiformal stack consists of multiple units. Namely the Rialp, Orri-, Nogueras- and Pallaresa unit. In between the Pallaresa and Nogueras unit lies the Llavorsi-syncline, which is part of the Pallaressa thrust-sheet. All are east – west trending structures. (see figure 1) (*Choukroune, 1992*).
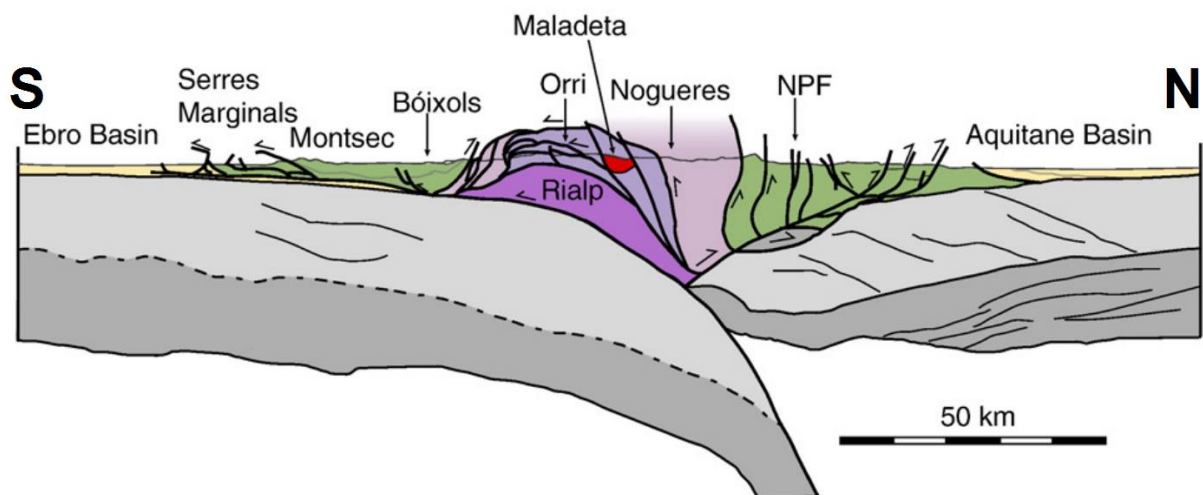

Figure 1, Schematic cross-section of the Pyrenees along the ECORS-profile (Metcalf, 2009).

3. Tectonic evolution of the Pyrenees

The Pyrenees lie on a convergent boundary between Iberia and Eurasia, which is mainly controlled by the counterclockwise rotation of the Iberian Peninsula in relation to Europe, due to the opening of the Bay of Biscay (*Vissers, 2012*).

The mountain-range itself resembles an asymmetrical double vergent tectonic wedge (*Sibuet, 2004*). The formation of the Pyrenees (see figure 2) started in the early Cretaceous, where until late Aptian there was a transtensive deformation phase of the already narrow Tethys ocean (*Lagabrielle, 2010*) (see figure 2a). From late Aptian until late Albian the Neo-Tethys subducted and back arc basin extension created a back arc basin on the Eurasian plate; the Aquitane basin. The Northern Pyrenean Fault (NPF) is considered the plate boundary between Iberia and Eurasia (*Zwart, 1986*). The NPF is an alpine structure that has accommodated hundreds of kilometers of strike slip displacement (*Le Pichon, 1971*), but the nature of the NPF is still subject of discussion (*Zwart, 1986*). Geophysical evidence indicates that there is a large offset in the depth of the Mohorovicic-discontinuity underneath the NPF, which suggests that the NPF is vertical and goes deep into the mantle (*Daignieres, 1982*). Around 80 Ma the opening of the Bay of Biscay, which thrived the rotation of Iberia (*Vissers, 2012*), ceased (*Sibuet, 2004*).

These movements are confirmed by paleomagnetic data (*McCaig, 1984*) which revealed that Iberia moved with relation to Eurasia from 140 to 100 Ma in a South-West direction, subsequently it moved to the East for 400 km from 100 to 75 and at last from 75 onwards to the north-west. These movements resemble the rotation of Iberia (*Vissers, 2012; Sibuet, 2004*). Apatite fission track data indicate that the maximum uplift of the Pyrenees took place during the middle Eocene to middle Oligocene (*Fitzgerald, 1999, Metcalf 2009*). The overall crustal shortening of the Pyrenees is estimated by reconstructing the ECORS cross-section (*Choukroune, 1989*) and paleomagnetic data (*Roest & Srivastava, 1991; Olivet, 1996*) and shows shortening between 120 and 160 km with the amount of shortening decreasing in westerly direction. The duration of the main shortening in the Pyrenees has been estimated to be 60 Ma, which gives a shortening rate of 2.5 mm/yr (*Zwart, 1979*). Similar shortening rates have been found elsewhere in the Pyrenees (*Vergés, 1995*).

4. Axial Zone of the Pyrenees

The Axial zone consists of Paleozoic meta-sediments where two main structural domains can be distinguished: a low grade supra-structure with steep folds and foliation with crenulated bedding (*Zwart,* 1979) and a high grade infrastructure with small-scale parasitic recumbent folds and near horizontal foliations (*Zwart, 1986*). The Axial Zone consists of several large structural units, namely the metamorphic massifs (such as the Aston-Hospitalet, Canigou and Lys-Caillaouas), the North Pyrenean massifs, the Nogueras zone and granite/granodiorite massifs (e.g. the Maladeta).

The foliations of the low grade meta-sediments have a decreasing dip to the South, creating a large fanning structure, which is related to the Alpine deformation phase (*Zandvliet, 1960*). These low grade rocks show metamorphism up to upper greenschist facies (*Zwart, 1979*). Two large anticlinoral structures can be distinguished in the central Axial Zone: the Pallaresa anticlinorium in the North and the Orri-Payasso dome in the South. Between these two structures lies the Llavorsi-syncline; a tight to isoclinally folded ESE-WNW trending syncline, which runs from Andorra to the west where it is cut–off by the Maladeta grandiorite, which intruded around 300 Ma ago (*Zwart, 1979; Evans, 1998, Metcalf 2009, Yelland*), demonstrating that the folding of the Llavorsi-syncline is Variscan. The axial plane of the syncline dips 30-50 degrees to the North and many smaller scale folds (in the order of hundreds of meters and smaller) are parasitic to this main feature.

The southern limb of the Llavorsi-syncline shows a large thrust fault, which is situated in the weak and incompetent Silurian slates, causing it to be the décollement between the Cambro-Ordovician and Devonian. This weak property of the Silurian rocks is visible in the diapiric intruding behaviour of Silurian slates in the Carboniferous rocks (*Harteveld, 1970*).

On geologic maps, folds can be recognized with a N-S to NE-SW trend. Some of these structures featured interference of two folding generations (*Boschma, 1963; Mey, 1967, 1968*). Fieldwork revealed that the folds predate the main cleavage phase, since the foliation cross-cuts the N-S to NE-SW oriented folds in the Orri-Payasso dome (*Mey, 1967; Zwart, 1979*).

In comparison with the Maladeta granite, the metamorphic massifs in the Axial Zone are much older. The orthogneisses of the Aston-Hospitalet domes show U-Pb ages of 470 Ma (*Denele, 2009)*. The orthogneisses in the Canigou massifs show similar ages (*Denele, 2009; Cocherie, 2005*).
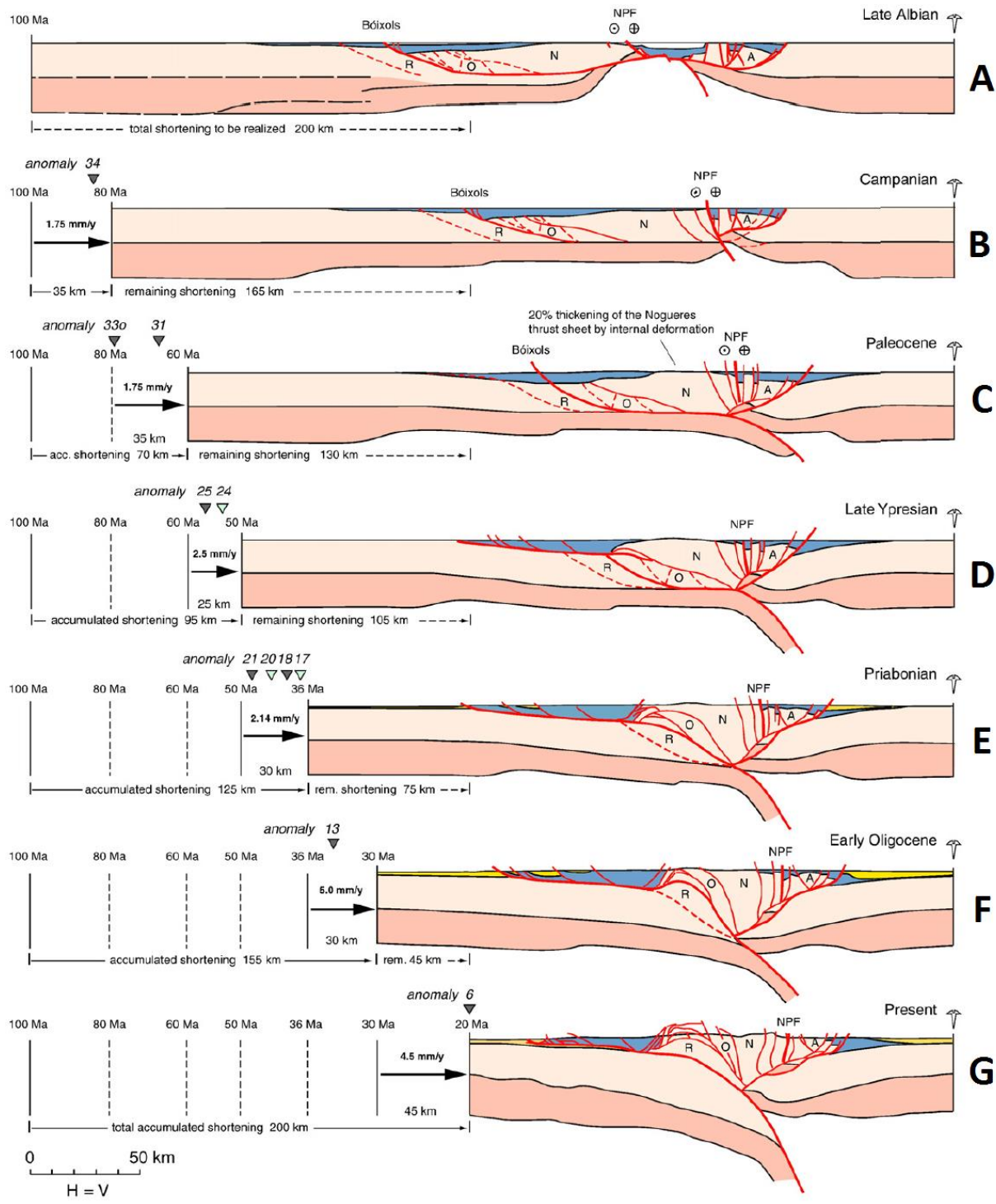
Figure 2, A balanced, partially restored cross-section of the crust along the ECORS Pyrenees profile, after Beamont et al. (2000). Note that the time scales shown upper left of each section are distorted (*Vissers, 2012*).

In the central Axial Zone there are two sets of cleavages to be recognized. One cleavage phase resulted in E-W striking foliation which always dips less than the main deformation phase cleavage. The other cleavage phase resembles NW-SE striking foliations with a steep dip (*Zwart, 1979*). The main phase deformation during the Variscan Orogeny is responsible for the main geometry of the Axial Zone (*Zwart, 1979)*. The age of the crenulation cleavages, is constrained by pebbles within Stephanian conglomerates that contain two cleavages (*Zwart, 1986*), indicating that some of the crenulation is of Variscan age. Alternetively, the middle Eocene-Oligocene conglomerates south of the Axial Zone, contain Mesozoic carbonates and Palaeozoic meta-sediments (*Rahl, 2011*), resulting from the Alpine uplift of the Pyrenees.

In the ECORS cross-section of the Axial Zone (see figure 1) all the mentioned structures comprise a general large feature of the Pyrenees: The Pyrenean antiformal stack, comprised of several southward facing thrust-sheets, which involve Variscan basement and an Upper Carboniferous to Triassic cover (*Zwart, 1979*). The antiformal stack consists of multiple thrust sheets: The lowest sequence of the stack is the Rialp thrust sheet, which is exposed in a tectonic window in the southern part of the central Axial Zone (*Muñoz, 1992*). Upsection, the Rialp thrust sheet is followed by the Orri thrust sheet, which is in turn overlain by Nogueras thrust sheet. The thrust structure is mainly a Variscan feature in the Axial Zone (*Muñoz, 1992*). During progressive deformation, the location of new thrust ramps behind the overlying thrust sheet resulted in forelandwards rotation of previous thrust sheets (*Zwart, 1979*).

4.1 Stratigraphy
4.1.1 Cambro-Ordovician
The Axial Zone consists mainly of Precambrian and Paleozoic rocks. Because there are no marker beds in the Cambro-Ordovician rocks, a correlation between the different lithologies has proven to be difficult. Zandvliet (*1960*) divided the Cambro-Ordovician in the Lleret-Bayau series and the stratgraphic higher Pilas-Estats series. The lower Lleret-Bayau series consists of an important limestone layer associated with black slates, quartzite layers and calcareous slates (*Zwart, 1979*). This series occur in the central Pyrenees, which is in agreement with the westward axial plunge of the Pyrenees, which is responsible for the exposure of the deepest rocks in the Eastern Pyrenees (*Zwart, 1979*). The Pilas-Estats series, according to Zandvliet (*1960*), consists of slates, quartzites, quarzitic slates and micro-conglomerates. On top of these series lies the Rabassa conglomerate. This conglomerate consists of pebbles of quartz, slate and occasionally black schist or gneisses in a matrix of slate. According to Harteveld (*1970*) this conglomerate resembles partially a mudflow. The main thickness of the Cambro-Ordovician is indicated as 2000 meters, but remains unknown, since no basement is exposed (*Zwart, 1979*).

4.1.2 Silurian
The overlying Silurian epoch is characterized by a very uniform deposition of black, carbonaceous shales. Due to its softness and incompetent behavior in deformation is has a profound influence on the topography and tectonic style of the structures in the region (*Zwart, 1979*).

4.1.3 Devonian
The Devonian strata have been divided into two subfacies (*Mey, 1968; Harteveld, 1970; Boersma, 1973*), namely the Sierra Negra subfacies and the Compte subfacies. The Sierra Negra consists of dark slates combined with limestones. The Compte subfacies consist of reddish slates with reddish, grey limestones (*Zwart, 1979*).

4.1.4 Carboniferous
The Carboniferous strata can be divided into a pre-Variscan and post-Variscan period. The pre-Variscan carboniferous (Dinantian to Westphalian) participated in major deformation during the Variscan orogeny. The Lower Carboniferous contains limestones interbedded with large black chert layers (*Zwart, 1979*). The post Variscan Upper Carboniferous rock units consist of sedimentary deposits interbedded with volcanics and lie unconformably on top of the lower Carboniferous (*Zwart, 1979*).

4.1.5 Permo-Triassic
Permian strata form the youngest rocks of the Paleozoic sequence within the Axial zone. Monotonous grey to red alternating mudstones, siltstones and sandstones interbedded with tuffs and dolomites comprise this sequence. The upper boundary of the Permian is defined at the sharp contact with the unconformably overlying Triassic Buntsandstein.

In some parts of the Axial Zone, Cenozoic conglomerates can be found, such as described by Rahl (*2011*) and Metcalf (*2009*).

4.2 *Variscan phases of deformation*
4.2.1   Structural style and kinematics
There are multiple phases of deformation recognized in the Axial Zone. Some extensional (*Vissers, 1992*) but mainly compressional.

The oldest compressional structures in the Axial zone predate the main phase of deformation (*Zwart, 1979*). Especially near the Northern and Southern border of the central Axial zone, the formerly mentioned N-S and NE-SW structures can be found (*Boschma, 1963; Mey, 1967, 1968*). This first generation of folds has steep axial planes. A later generation of folds show an E-W to NW-SE trending axial planes which dips to the NNE. More to the central part of the Axial Zone the trend of these second generation folds are more E-W trending, but there is still evidence for the F0 folds (*Zwart, 1979*). In the Llavorsi-syncline structures closed on both sides are found which have an elongated shape. These are probably flat dome or sheath structures, which is supported by the fact that the cleavage-bedding lineations are instead of

E-W trending lying within the cleavage plane and plunge to the North (*Hartevelt, 1970*).

The main phase of deformation (F1) is responsible for the main structures of the Axial Zone. It is difficult to trace out major folds, as marker beds do not exist in the monotonous quartz-phyllites of the Cambro-Ordovician, but the main phase has formed the large syn- and anticlinoria in the central Axial Zone and created the fanning of the foliation throughout the central Pyrenees (*Zwart, 1979*). This fanning is not gradual from north to south, but in several compartments the angle of the foliation suddenly changes (*Zandvliet, 1960*). This feature predates the intrusion of the Maladeta granites, as it is in contact with low dipping slates (*Zwart, 1979*). As the main deformation phase in the Variscan orogeny resulting in E-W trending structures. During this deformation phase also the Llavorsi fault, on the southern limb of the Llavorsi-syncline has been active (*Muñoz, 1992*). Its Variscan age can be demonstrated by the cross-cutting relationship with the Maladeta-granite and its contact metamorphic aureole (*Muñoz,* 1992). This fault has also been active during the Alpine deformation (*Zandvliet, 1960*). The structures mentioned by Vissers comprise of a crustal scale extension in the Pyrenees during Variscan times. This can be seen in the tilted halfgraben geometry of the Permian volcanics and terrestrial sediments which are deposited syn-tectonic with the Variscan orogeny (*Vissers, 1992*). Also inversion of Variscan several Variscan faults in the Axial zone is visible (*Losantos, 1986*).

After the main phase of deformation (F1), at least four deformation phases can be recognized (*Zwart, 1979*). The F2 post-dates the main phase slaty cleavage and schistosity. It has a sub-horizontal axial planes and N-S oriented fold axes (*Oele, 1966; Lapré, 1965; Zwart, 1963*). In the Aston-massif the folds very between open and isoclinal structures with a top S asymmetry (*Zwart, 1979*). These features are overprinted by F3 folds consisting of two distinctive sets (*Lapré, 1965; Oele, 1966; Zwart, 1963)*. One set, the F3a phase, has NW-SE striking folds with almost vertical axial planes. The F3b phase has NE-SW striking folds with very steep axial planes. These folds deform the compositional layering of the Paleozoic rocks (*Zwart, 1979)*. F3 folds are always accompanied by a well-developed crenulation cleavage (*Zwart, 1979)*. F4 folds are structures with an E-W striking

orientation with a steep axial plane. These can frequently be found in the Pallaresa anticlinorium.

4.2.2   Igneous activity and metamorphism

There are three phases of metamorphism in the Pyrenees: Pre-Cambrian, Variscan and Alpine. Pre-Cambrian metamorphic rocks can be found in some of the massifs in the Axial Zone, such as the St. Barthelemy, Castillon, Agly Arize and Trois Seigneurs (*Zwart, 1954, 1959*). Alpine metamorphism is only found in narrow zones in the Mesozoic sequences North of the Axial Zone in the North Pyrenean Zone. The Variscan metamorphism can be found in all pre-Late Carboniferous sediments, the Precambrian basement and the pre-Variscan granites (*Zwart, 1979*). In the Cambro-Ordovician, Silurian, Devonian and the Lower Carboniferous low grade metamorphism is recorded within slates and phyllites. The foliation of these rocks are parallel to the axial planes of the F1 folds from the main phase deformation. The minerals found in these metamorphic rocks are mainly quartz, mica's, chlorite and chloritoid. These minerals indicate a lower greenschist facies (*Zwart, 1979*). Especially chloritoid is very abundant in the slates of the Carboniferous in the Llavorsi-syncline. Occasionally chloritoid is encountered in Cambro-Ordovician and Devonian slates (*Zwart, 1979*). In the South of the Axial Zone, for example in the Cambro-Ordovician rocks near Seo d'Urgell, even lower metamorphic facies can be found. Around the metamorphic and granitic massifs, like the Canigou and Hospitalet, rocks of amphibolite grade metamorphism are present. In the Axial Zone there are multiple metamorphic zones identified of Variscan age (*Zwart, 1979*). Zone I consists of chlorite, muscovite and chloritoid. Zone II contains biotite, muscovite, andalusite and corderite. Zone III is similar to zone II, but also contains the staurolite. In zone IV the andalusite is transformed in silliminite. The last zone, zone V, contains then biotite, corderite, silliminite and K-feldspar (*Zwart, 1979*).

4.3 Alpine phases of deformation
4.3.1   Alpine structures within the Axial Zone
The Variscan structures of the Axial zone underwent an Alpine overprinting. These Alpine structures in the Axial zone can be recognized as brittle deformation features, which strike parallel to the main Variscan structures (*Zwart, 1979*).
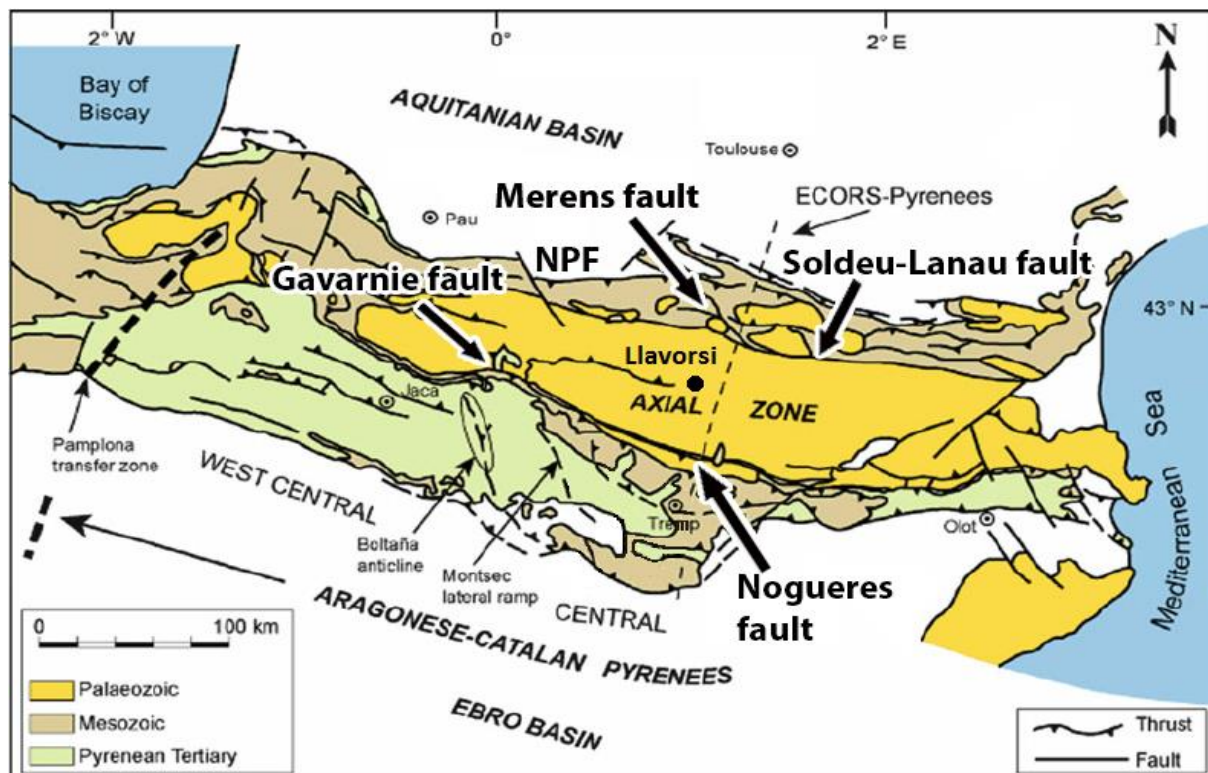
Figure 3, A schematic geologic map of the Pyrenees, showing the location of Llavorsi in the central Axial Zone, and the major geologic structures. (Modified after *Martinius, 2012* and *Rahl, 2011*)

Besides brittle deformation, the Alpine phase also resulted in folding of the Variscan foliations. Especially the southern part of the Axial Zone is quit evidently influenced by Alpine folding. Alpine cleavages are found to be present in Paleozoic rocks (*Seguret, 1970; Muller, 1977; Majesté-Menjoulas, 1979*). The formerly mentioned F4 deformation phase is most likely of Alpine age in the Orri-Payasso dome (*Zwart, 1979*).

Examples of the Alpine structures can be found on the borders of the Llavorsi-syncline. Although not well exposed, the weak Silurian slates form the decollement for the Llavorsi-fault on the southern border of the Llavorsi-syncline, which has been active during the Alpine orogeny (*Zandvliet, 1960*). To the North of the Llavorsi-syncline lies the Mérens-fault (see figure 3). A strike slip structure and together with the Llavorsi-fault, Gavarnie-fault, Soldeu-Lanau-fault and the Nogueras-fault, it resembles one of the main faults in the Axial zone of Alpine age.

4.3.2 Tectonic framework

During the Alpine Orogeny, the Axial zone was involved as a block in the convergent plate motion of Eurasia and Iberia. The former foreland basins on both the Northern and Southern side of the Axial zone became major thrust belts. Whereas certain large faults, such as the NPF and the Merens fault, showed mainly strike slip behavior (*Zwart, 1986*).

4.3.3 Age constraints on Alpine structure

Fault gouges samples of several Alpine structures has been taken to study the age of these structures (*McCaig, 1986; Rahl, 2011*). Ar-Ar dating of illite in the fault gouge of major Alpine faults (see figure 3) shows that the faults have been active around 90-50 Ma (*McCaig, 1986, Rahl, 2011*). Other measurements using Apatite fission track analysis show that the Maladeta-massif underwent continuous exhumation during the Alpine orogeny, showing AFT-ages of 30 Ma, resulting in a 0.2 mm/yr exhumation rate (*Metcalf, 2009*). Zircon (U-Th)/He dating by Filleaudeau in 2012 shows an exhumation rate 0.4 km/Ma in the late Cretaceous and 0.2 km/Ma up to the middle Eocene (*Filleaudeau, 2012*), which is in the same order of magnitude.

5. Results

Field data has been acquired from 52 locations in the Spanish Central Pyrenees (see appendix 9). In this report the kinematic and petrological aspects of the collected data and samples will be described and discussed.
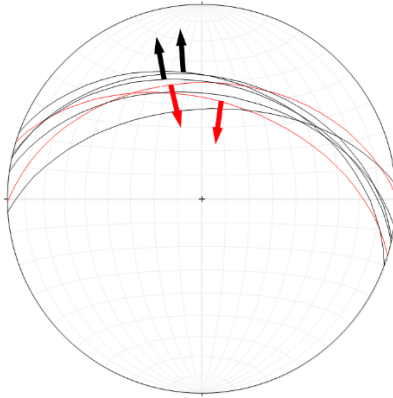
Figure 4, Showing the measurements of the rocks in figure 18.1. The red great circles are measured on the contact between the Devonian and Silurian strata, which resembles the fault plane. The red arrows are striation directions and the black arrows are stretching lineations. The black great circles represent the measured S0 and S1.
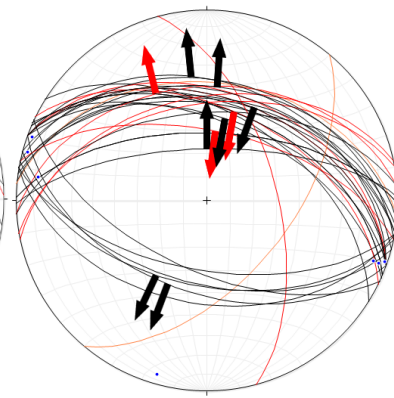
Figure 5, A stereographic projection of the measurements in the Llavorsi-area. The black great circles indicate (foliation) planes with the S0 and S1 dipping to the NE and the sub-horizontal S2 dipping slightly to the NW. The black lines dipping to the SW are measured kink-bands. The red great circles indicate faults, and the orange great circles resemble Riedel faults. Red arrows are striations and black arrows are stretching lineations
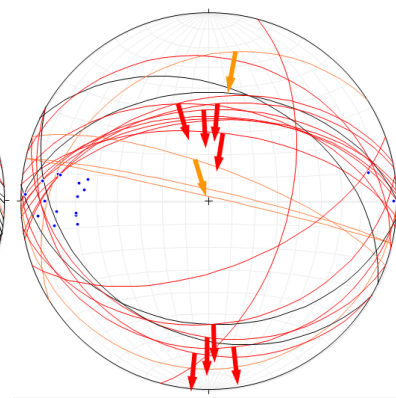
Figure 6, Showing the measurements of the Vall de Fosca. In black, the S1 foliation is shown, in red the faults are shown with their striations shown as black dots and the Riedel shears in orange.
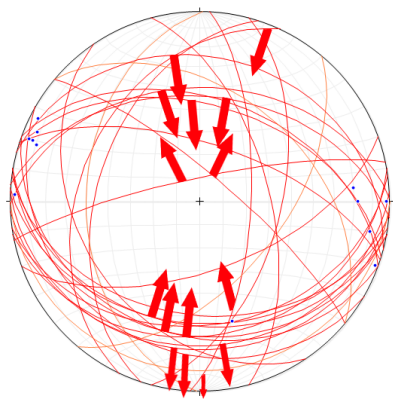

Figure 7, showing the faults measured in the Devonian rocks of the Llavorsi-syncline. The black dots resemble the striations measured on the fault planes and the blue dots resemble the measured fold axes.
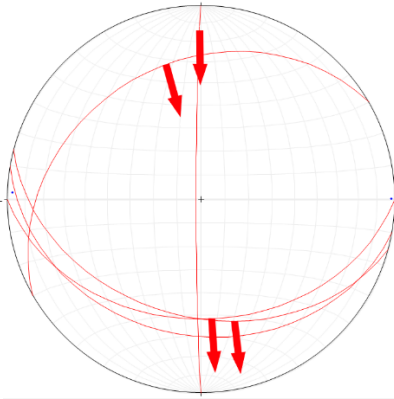
Figure 8, showing the faults and striations of the Permo-Trassic rocks in field area.
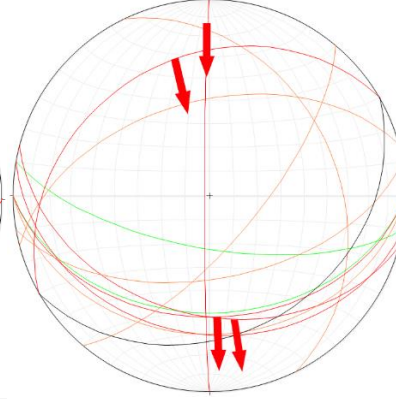
Figure 9, Showing the measurements of the Port del Canto region with the Permo-Triassic bedding in green, the faults in red with the striations indicated by the red arrows. Riedel faults are visualized in orange.
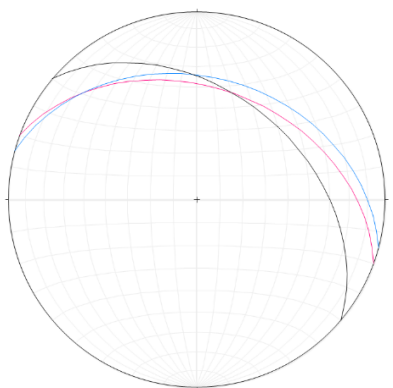

Figure 10, A projection of the measurements of location 36, near Tirvia, with in pink the S0, in blue the S1 and in black the S2.
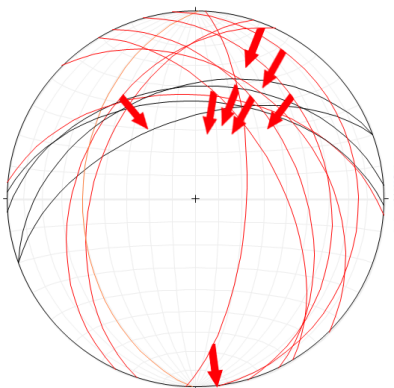
Figure 11, showing the measurements of the Vall d'Aran. S1 foliations are shown in black, faults in red, Riedel shears in orange and the striation directions are indicated by the red arrows.
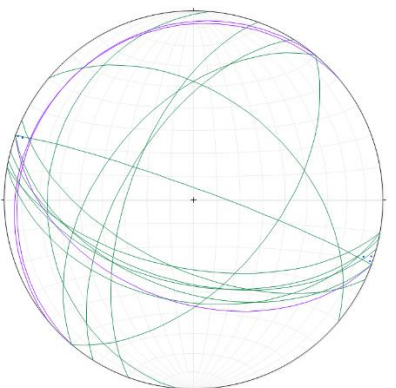
Figure 12, Stereographic projection showing in purple the measured shear-bands and in green the kink-bands in the Devonian and Carboniferous rocks around Llavorsi and in the Vall de Boi.
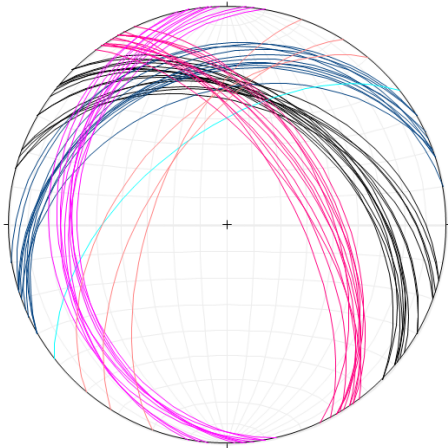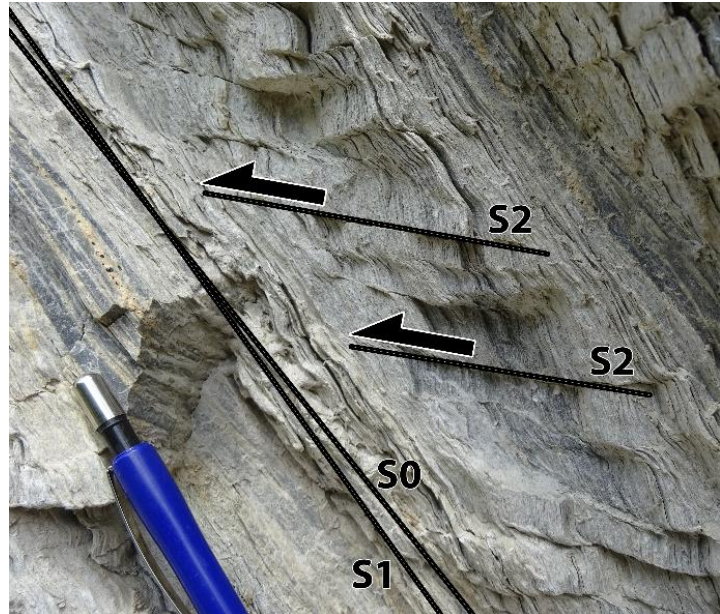
Figure 13, showing the measurements of S0, S1 and S2 structures in the Vall de Boi. The measurements are plotted as follows:

Devonian S0   :   Black   great   circles
Devonian S1   :   Blue   great   circles
Devonian S2   :   Cyan   great   circles
Carboniferous S0 :   Pink   great   circles
Carboniferous S1 :   Purple   great   circles
Carboniferous S2 : Light pink great circles

^ Figure 14a, showing the shear-bands in the Devonian rocks at location 33. It shows clearly that the S1 is cross-cutting the S0 at a very shallow angle and that the S1 foliation is crenulated by a sub horizontal C^1 foliation which is confined to a discrete zone of 5cm

^ Figure 15a, Showing the bottom of the Maladeta-granite with the contact to the pink deformation band indicated by the black line. As indicated by the arrow, there are small shear-zones within the granite with a top south shear sense, similar to the adjacent mylonite zone underneath.

^ Figure 14b, showing the kink-bands in the Devonian rocks at location 33. The Kink-bands are found in green rocks which hold a lot of chlorite, mica and calcite. They are not found throughout the whole sequence. The C^1 foliations dips around 45 degrees to the south and shows a top south shear sense.

< Figure 15b, The contact between the Devonian hornfels at the bottom and the Maladeta-granite on top, showing ductile behavior. Both the granodiorite and the defomation zone show foliations

9

5.1 Field observations

The field observations of the Spanish Central Pyrenean area, in the Pallars Sobirà, Northern Pallars Jussà and Alta Ribargorça regions, including orientations of faults, folds, foliations, stretching lineations and striations. Samples of formations ranging from Cambro-Ordovician to Cretaceous ages have been taken to the lab for further petrologic analysis.

5.1.1 Kinematic field-description

The measured major structures in the Pallars Sobirà, Northern Pallars Jussà and Alta Ribargorça area, which are the Llavorsi-syncline, major faults like the Nogueres-fault and Llavorsi-fault and the S1 foliation, show a general ENE-WSW trending strike of the folds, faults and foliation. In the Llavorsi-syncline area the penetrative foliation is an axial plane foliation of the isoclinally folded Paleozoic stata (S1) (*see figure 5*). This axial plane foliation has an ESE-WNW strike, dips at an angle of 50° to the North and has been crenulated by a second axial plane (S2). This S2 foliation folds the S1 foliation, but is not developed throughout the whole region. This S2 foliation is only visible in certain Cambro-Ordovician, Devonian and Carboniferous rocks (locations 8, 33, 36 and 39 in appendix 9). Now we will discuss the measurements in more detail for every region within the fieldwork area, see appendix 1 for locations. Measurements of the structures in Devonian rocks in the Llavorsi-area, which are situated on the southern limb of the Llavorsi-syncline (locations 28 up to 33), are shown in a Schmidt-stereographic projection in figure 5. It clearly shows the ESE-WNW striking penetrative foliation (S1). In these Devonian rocks (locations 28 up to 33 on appendix 1) there are kink-bands and shear-bands present (see figure 14a and 14b). The shear-bands are confined in multiple small discrete zones around 5cm wide and show a top south shear sense. These discrete zones are parallel to the S1 foliation. The C[1] shear planes created by the crenulation of the S1 foliation in these zones are sub-horizontal (Figure 14a). The kink-bands in the Devonian rocks near Llavorsi show also top south movement (see figure 14b). Furthermore, the orientations of the kink-bands and shear-bands are non-consistent. Some of the kink- and shear-bands in the Devonian and Carboniferous show an equal strike, but dip either to the north or south, whereas other kink- and shear-bands cross-cut the S1 in a plane which is very flat-lying. This is seen in figure 12, which shows the orientation of the kink-bands and shear-bands in the Devonian and Carboniferous rocks. The Devonian on the northern side of the Llavorsi-syncline, near Tirvia (location 36 and 38), shows a S1 foliation which has the same orientation as the S1 on the southern limb of the syncline. In the northern area, the bedding of the Devonian strata is visible as well as in the southern limb. The orientation of these rocks in the northern limb displayed in figure 10. The S2 has however a different orientation than in the south. Whereas the shear-band foliation had a sub horizontal orientation in the south, in the north the S2 foliation has a NW-SE orientation and a slightly steeper dip, as is displayed in figure 10.

In the Vall d'Aran (locations 1 up to 4), we find the main foliation to have an ENE-WSW orientation and dips around 50 degrees to the north. Many of the faults in this valley show a general N-S strike, having a large top south strike slip component with striations plunging around 30 degrees to the NE. A few faults show an EW strike, with a similar direction of the striations. Results of the Vall d'Aran can be seen in figure 11. In the Vall d'Aran, the contact between the Maladeta-granite and the Devonian rocks is well exposed (location 2). The Devonian rocks have been turned into hornfels via contact-metamorphism due to the presence of the Maladeta-granite. The contact itself consists of a purple band which is 30 centimeters thick, where localized deformation has taken place (see figure 15a and 15b). Figures 15a and 15b show that there ductile deformation has occurred in this pink layer, which consists of deformed quartz, k-feldspar and muscovite from the Maladeta-granite. The thin-section of these rocks will be discussed later. This ductile behavior is also seen south of the contact (location 3) where hornfels boudins are asymmetric and separated by shear-bands with top south kinematics. There are also small shear-zones with a top south shear sense and stretching lineations plunging to the NNE found on S1 foliation planes near pinch and swell structures within the limestone, as is displayed in figure 16. The stretching lineations lie parallel to the hornfels boudins in the limestone. In the Vall de Boi (locations 5 up to 10), east of the Vall d'Aran, orientation of the foliations is different. In figure 13 the measurements are shown of the Devonian and Carboniferous in the Vall de Boi. As shown in figure 13, the orientation of the bedding (S0) is more NW-SE trending as in the Llavorsi-area. The main foliation (S1) has in the Carboniferous almost a N-S orientation, dipping at a low angle to the west and the S1 in the Devonian has a more NE-SW strike,
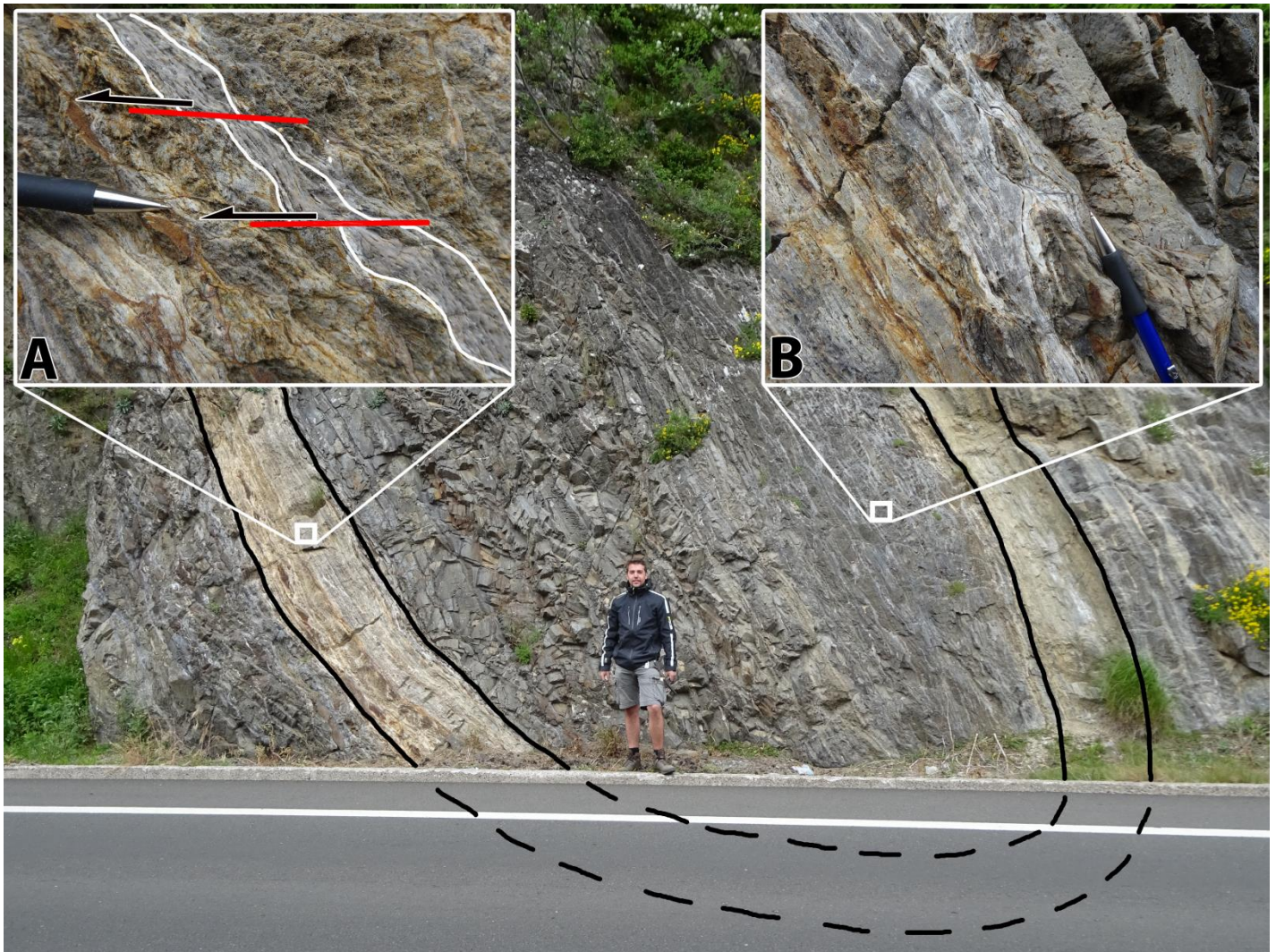
Figure 16, Showing a large structure in the Vall d'Aran in the Devonian hornfels. Within the light colored highlighted band there are small limestone boudins with little shear-bands separating the different boudins, as can be seen in figure 16a. Figure 16b shows a detail in between the two limbs, where hornfels boudins are separated by shear-bands with top south kinematics. The field of view is to the west.

dipping at a similar angle to the NW. The S2 foliation has in both the Carboniferous and the Devonian a NE-SW striking orientation with a small angle to S1, dips round 56 degrees to the NW and crenulates S1. In the southern part of the valley there is an unconformable contact between the Carboniferous and Devonian rocks with Triassic rocks. The nature of the unconformity is an erosive surface on top of which the Triassic rocks were deposited. The Triassic rocks have an E-W trend, dipping very steeply to the north (*see figure 13*). These layers show coarsening upward sequences to the south, whilst dipping slightly to the north, indicating overturning of the strata.

In the Vall Fosca, east of the Vall de Boi, the orientation of the main foliation (S1) has a strike which has a WNW-ESE orientation. The foliation dips however around 50 degrees in some cases to the north, and other cases to the South. The thrust faults in this region show similar orientations to the S1 with roughly N-S striation with a top south shear sense. The results of the Vall Fosca can be found in figure 6.

The Port del Canto region, to the South of the Llavorsi area (locations 45 up to 52) shows structures in Permian and Triassic rocks. These rocks are post-Variscan, so all the structures visible in these sequences are of Alpine age. The thrust faults show mainly an E-W strike with a dip of around 35 degrees to the south. Striations are indicating a top to the south movement along these faults. There are also a few N-S orientated faults with a strong strike slip top South movement, like the other faults. The measurements of the Port del Canto region are found in figure 9. The figure also includes the contact between Triassic rocks and the overlying Devonian rocks. The position of the Devonian rocks on top of the Triassic rocks is due to a large thrust at the base of one of the thrust sheets in the

antiformal stack in the southern Axial Zone, mentioned before. Due to extensive tilting this thrust now has an apparent normal shear-sense to the south. The shear sense of this fault prior to tilting was top south. All the faults in the studied area predominantly show shear-senses indicating thrusting with a top to the south movement. A few faults showed kinematic indicators such as rotated clasts and slickensides which suggested a top north shear sense of the fault, such as the fault in the Silurian on the Northern limb of the Llavorsi syncline, near the junction to Tirvia (location 37). On the Southern limb of the Llavorsi-syncline there is, according to Zwart, 1979, also Silurian strata present between the Devonian rocks of the Llavorsi-syncline and the Cambro-Ordovician rocks of the Orri-Dome. Furthermore, there is an excellent exposure of Silurian rocks, which can be found at location 23 on appendix 1, near the town of Baiasca. Thus far this is the only place where the Llavorsi-fault in the Silurian strata of the southern limb of the Llavorsi-syncline is exposed. An image of this exposure is shown in figure 18. The Llavorsi fault at this location shows similar orientations of the S1 foliation as in the Devonian strata near Llavorsi. The fault has an E-W to WNW-ESE trend and striations show a top south direction of movement. Shear sense indicators such as slickensides show a reverse shear sense of this major fault. Measurements of this Baiasca exposure can be found in figure 4. The Silurian in the Llavorsi region is easily distinguishable as they comprise of thin zones of black slates which have been heavily deformed. The movement on both sides of the Llavorsi-syncline, along the limbs have, mainly been accommodated by these Silurian black slates.

Figure 5 shows the S1 axial plane foliation of the Llavorsi-syncline and figure 7 shows the faults measured in the Devonian. The striations and stretching lineations plunge in general in an NNE to NE direction. As mentioned before the general movement along these faults is reverse. The striation structures however show a large scatter in figure 17. The plotted fold-axes are consequent with the measured faults and direction of the Llavorsi-syncline as we can conclude its orientation from the S1 foliation.
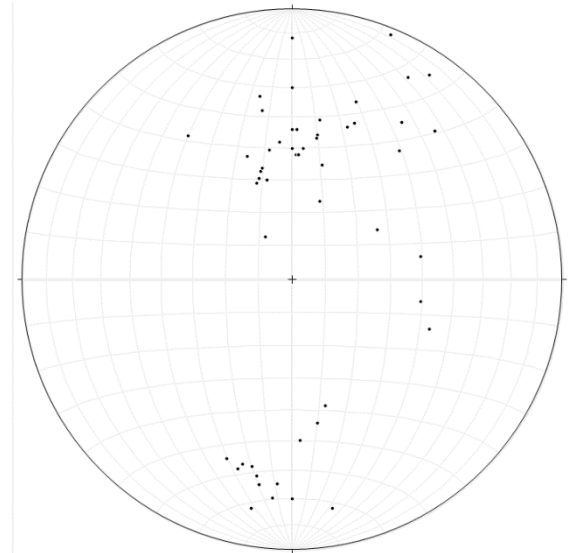
Figure 17, A stereo-plot showing the striation and stretching lineation measurements in the Llavorsi region. The directions of the lineations clearly show a distinct scatter as the structures do not line up in a discrete zone of movement.
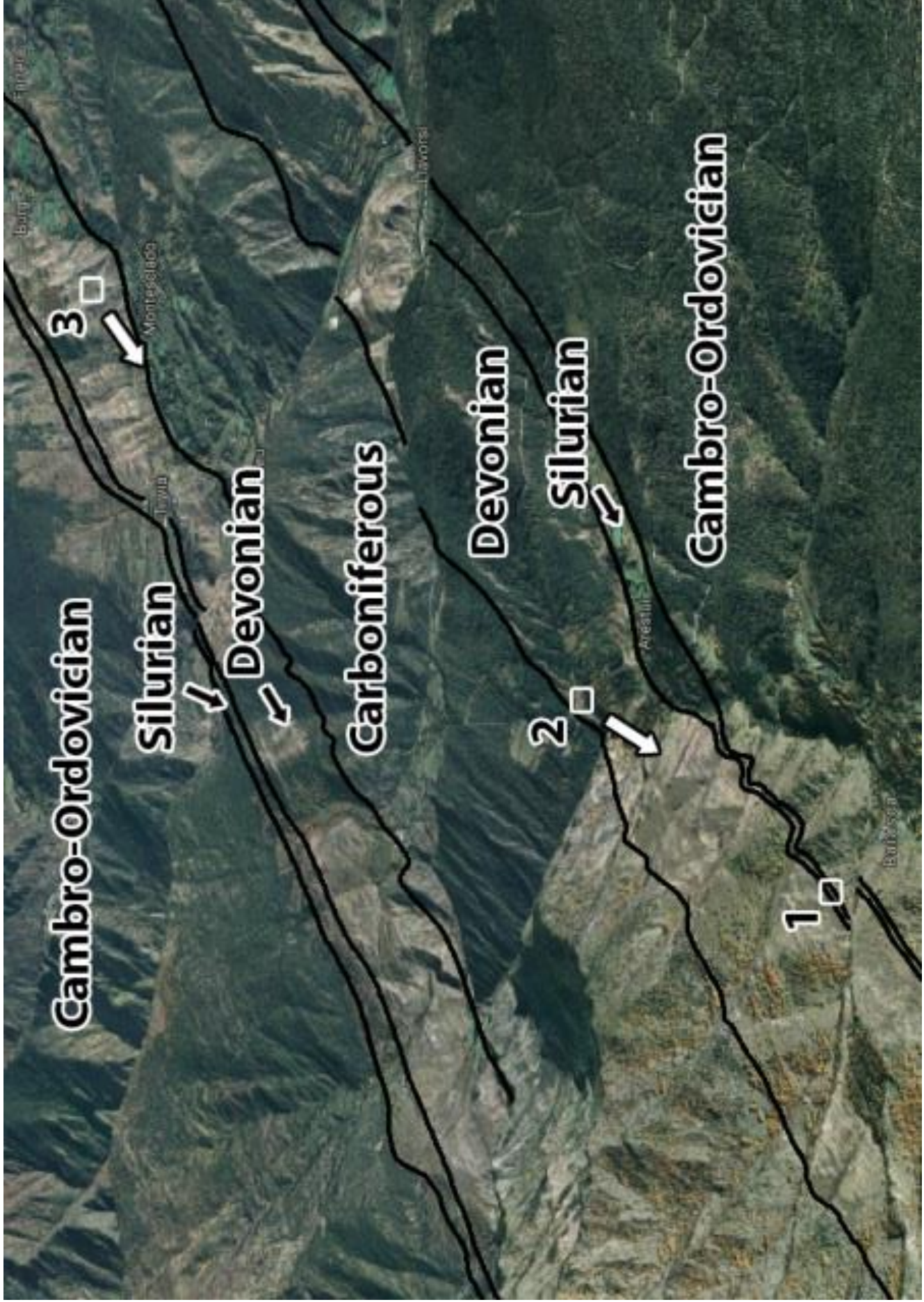
Figure 18, A birdseye view of the Baiasca location, at point 1. An image of this location can be found in figure 18.1. Images of the view in the indicated direction from locations 2 and 3 can be found in image 18.2 and 18.3. The field of view is towards the north-east (*Source: Google Earth*)
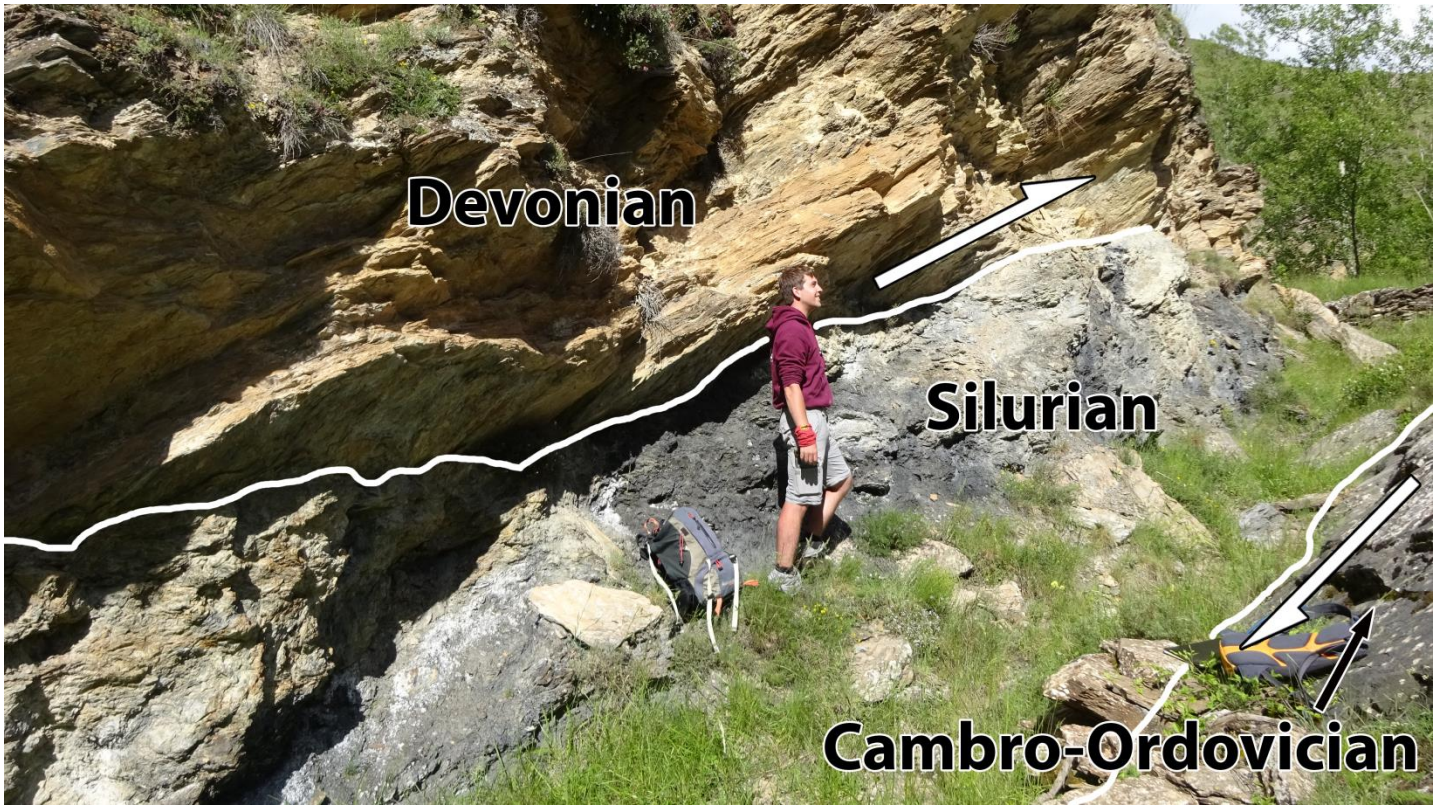
Figure 18.1, An image showing the exposure of Silurian rocks of the Southern limb of the Llavorsi-syncline near Baiasca. The incompetent black shales of the Silurian act as the fault zone in this system. The white arrows indicate the movement along the fault. The field of view is towards the east.
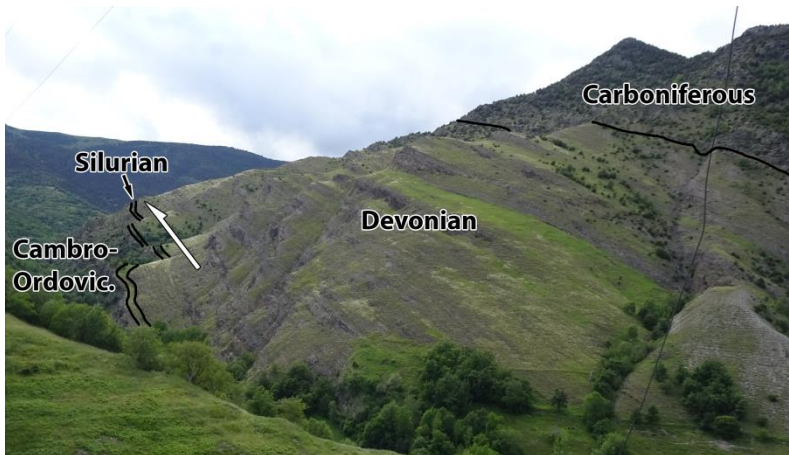

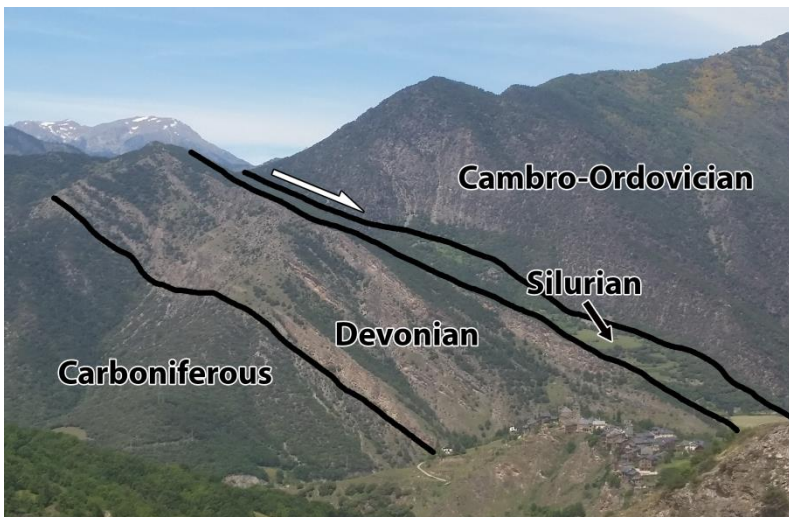Figure 18.2, View on the southern limb of the Llavorsi-syncline. The field of view is towards the west.

Figure 18.3, View on the northern limb of the Llavorsi-syncline. The field of view is to the west.

In the post-Variscan rocks of the Permian and Triassic we find structures which have slightly different orientation, also these rocks lack the presence of the S1 foliation we see in the Paleozoic rocks. The Mesozoic sequences do not show any foliation in this area. The thrust faults in these rocks are more EW orientated by 10 to 15 degrees compared to the previously mentioned rocks, as we found in Port del Canto region. These structures show a more discrete area in which the striation structures are plotted in a stereonet (figure 8). Also the fold axes have a distinct E-W trend in relation to the more ESE-WNW trend of the Paleozoic rocks. The measurements of these Paleozoic rocks can be found in figures 5 and 6.

5.1.2 Petrological field-description

In appendix 1, the locations which have been visited during the fieldwork can be found. Samples have been taken at the indicated field-locations on this map. The thin sections made from these samples show deformation of internal structures which indicate the pressure and temperature at time of deformation. First an overview of the mineralogical content is given.

The main rock forming mineral of the region is muscovite, combined with quartz and calcite. These minerals are found throughout the whole fieldwork area and comprise the main composition of the sampled rocks.

Cambro-Ordovician

The rocks of the Cambro-Ordovician in the fieldwork area, which can be seen on the geological map in appendix 8, are mainly resembled of dark grey colored phyllites containing quartz, sericite, pyrite, feldspar and calcite. The rocks itself were heavily deformed and shows a strong S1 foliation mentioned before.

Silurian

In the Llavorsi area the Silurian rocks are not very well exposed. Outcrops at Tirvia, Baiasca, Llessui and Boi reveal the lithology of the Silurian in the region to be largely the same black slates. The Silurian consists of very dark grey to black slates with abundant calcite and quartz veins in them documenting intensive folding and faulting. The slates contain organic material and graphite. The main mineral composition in the Silurian slates is quartz, calcite, pyrite and mica's such as for example muscovite.

Devonian

The Devonian rocks in the region consist mainly of quartz and mica minerals making up light coloured shales. These light coloured shales are the oldest layers of the Devonian and also contain crinoid fossils. In a few darker layers, the quartz veins are present containing pyrite minerals. These veins are heavily deformed. The darker rocks itself show signs of mylonitisation. In some layers chlorite is abundant, which coexists together with fine grained mica, calcite and quartz.

Carboniferous

The Carboniferous rocks in the studied area are mainly found in the central part of the Llavorsi-syncline and near Erill Castell. In the Llavorsi-syncline the rocks comprise of grey quartz rich schists and shales, containing pyrite and calcite as well. Furthermore, there are volcanic deposits of carboniferous age in the Erill Castell area. These volcanoclastics are made up of light coloured tuffs containing volcanic bombs.

Permo-Triassic

Permian and Triassic rocks are only found in the Southern part of the Axial Zone, in the Port del Canto region (see appendix 9). The rocks consist of red sandstones and shales containing a lot of muscovite. Within the Triassic, we find the Buntsandstein, which is represented throughout Europe. This distinguishable layer contains greyish-red sequences of conglomerates, coarse-grained quartz-rich sandstones and silt- and mudstones.
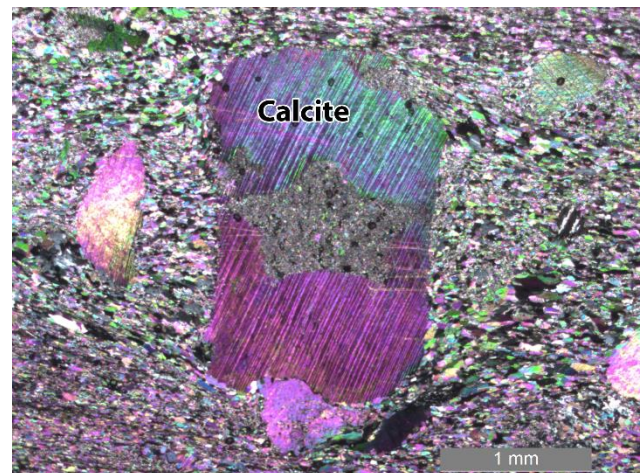

Figure 17.1, An image made in XPL of a calcite mineral in a matrix of muscovite and quartz showing 1st order twinning. The star shape in the middle is due to recrystallization of a pentacrine fossil.
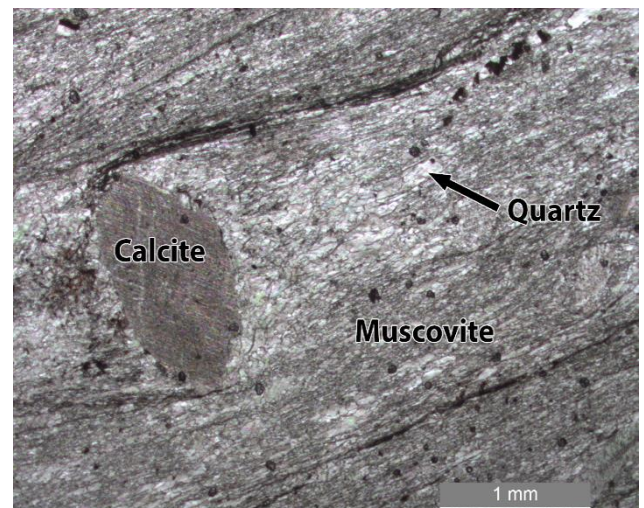

Figure 17.2, An image of a calcite mineral where it is visible that the pressure solution seems (dark black band) wraps around the mineral.

Microstructures

In appendix 9, the locations can be found where samples have been taken. These samples have been made into thin-sections which are studied under a light-microscope and a scanning electron microscope. An overview of all the samples is given in appendix 1. The most notable observations are mentioned here.

Samples 5.1.1 and 5.1.2 were taken from the Devonian in the Northern limb of the Llavorsi-syncline (location 36 in appendix 9). In these samples, we find a penetrative foliation parallel to the dark pressure solution seems in the thin-sections (*see figure 17.2*). Besides these seems there are multiple larger grains of calcite with distinct twinning patterns, which grain rotation also indicate a dextral shear sense. As can be seen
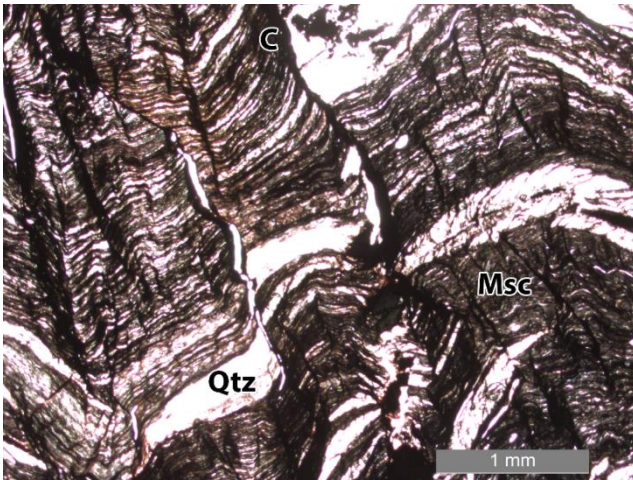
Figure 18, showing a PPL image of Silurian sample 6.4 containing muscovite, graphite and quartz with brittle deformation structures.
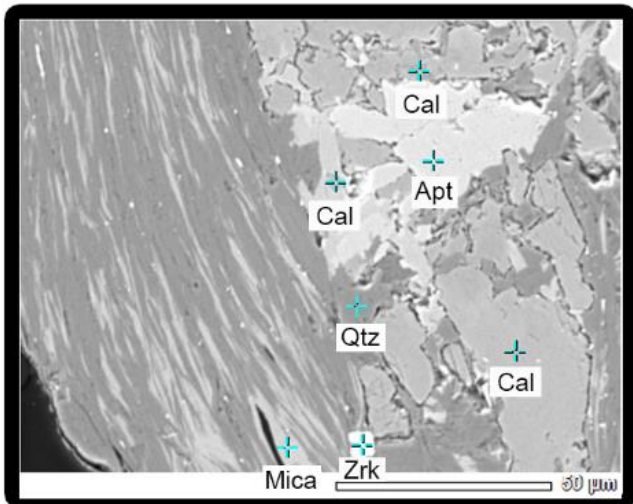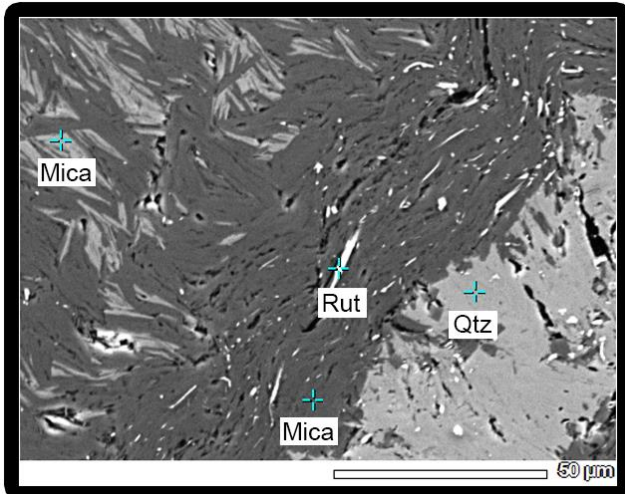

Figure 19a (above) and 19b (below) show SEM pictures indicating the present mineral assemblages in sample 6.4 and 6.4.1. As mentioned, the Silurian samples contain zircon (Zrk), calcite (Cal), quartz (Qtz), apatite (Apt), rutile (Rut) and mica's.

in figures 17.1 and 17.2, they consist of very twins with narrow spaced lamellae in a mineral that

shows high order birefringence. The twinning is of type I (*Burkhard, 1993; Ferill, 2004)* and the twin-lines in these samples have an average width of 3,5 micron and an density of around 40 twins/mm.

Samples 6.4 and 6.4.1 are from the Silurian, near Boi (location 7 in appendix 9). The thin-section shows a strong foliation in mica-rich parts, which are crenulated and folded on a very small scale (see figure 18 and 21). It also shows brittle deformation in some areas, like in figure 18. There are different types of mica present, like biotite and muscovite. in these rocks, which can be seen from the SEM results. In this mineral, SEM results also revealed that there is rutile and zircon present in very small minerals (see figure 19). Furthermore, there was organic material present in these Silurian rocks in the form of graphite and pyrite. These pyrite minerals had asymmetric fringes on either side, containing calcite (see figure 20).

Samples 7.3.1 and 7.3.3, from location 2 in the Val d'Aran shown in figure 22.1 and 22.2, taken just underneath the Maladeta-granite, reveal intense deformation has occurred on the contact between the Maladeta-granite and the underlying Devonian hornfels. The thin-section from this mylonite zone shows dynamic recrystallized quartz, showing a lattice preferred orientation. Sample 7.3.3 even shows ductile deformation of quartz and muscovite minerals, which originate from the Maladeta-granite. The thin-sections also show brittle deformed K-feldspar minerals (see figure 22.2). Some K-feldspar minerals have been converted into very fine grained mica's by a process called saussurization. The samples are mica- and quartz rich, forming the major foliations in the rock. Biotite minerals has been replaced into chlorite minerals, which happened post magmatic due to present fluids. The foliated quartz and mica's wrap around calcite and chlorite minerals and reveal together with mica fishes a top to the south shear sense.

In sample 8.5, from the Devonian shear-bands (see figure 23) in location 33, we find a spaced S1 foliation of mica's and calcite, which is crenulated to form the shear-bands, we mentioned before. The thin-sections contain calcite minerals and monazites, zircons and pyrite. The thin-section also reveal the top to the south shear-sense of the shear-bands.

In sample 10.8.2 from the Silurian fault-zone in the southern limb of the Llavorsi-syncline, found near Baiasca (location 23), a deformed rock can be seen. This fault breccia shows even on micro-scale intense deformation, as shown in figure 24. Microscpical analysis with the gypsum plate shows that the quartz minerals show a
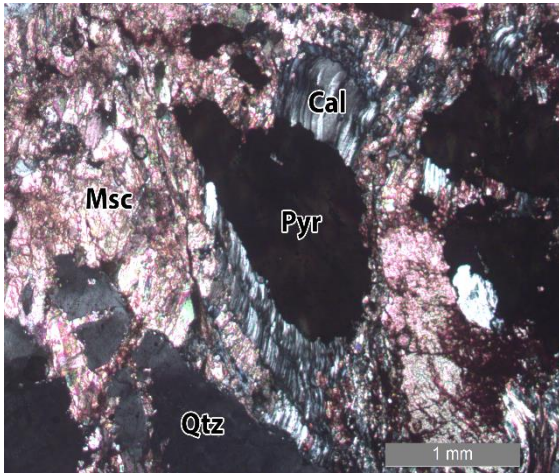
Figure 20, An image in XPL from sample 6,4 showing a pyrite mineral with asymmetric calcite fringes on either side of the mineral. The orientation of the fringes is parallel to the microstructural folding of the Silurian rocks (see figure 21)
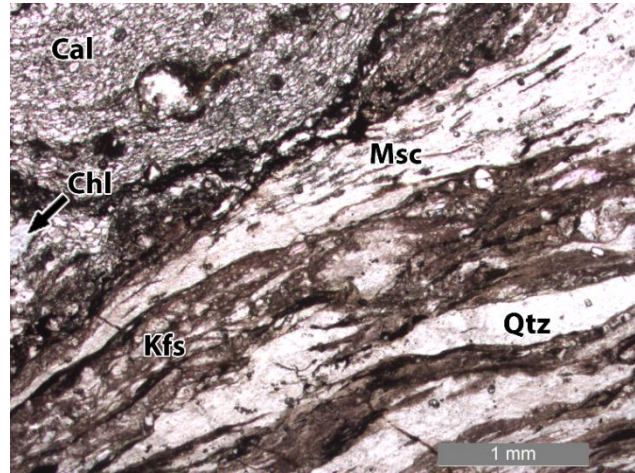

Figure 22.1, Showing an image of the contact between the Maladeta granite and the Devonian hornfels. The bottom right corner shows ductile deformation in the quartz and muscovite, whereas the K-feldspar shows brittle behavior.
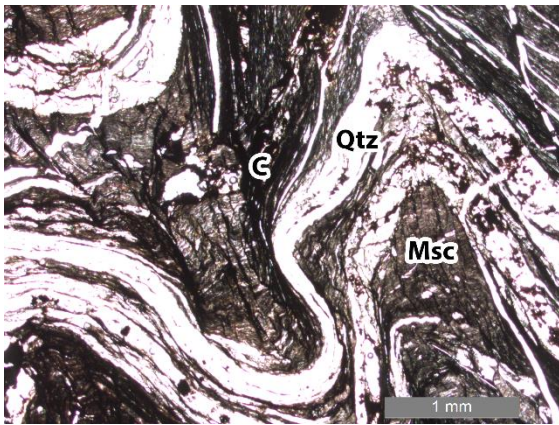

Figure 21, An image in XPL of Silurian rocks from sample 6.4 showing the micro-scale folding of these rocks.

Figure 22.2, showing a calcite mineral in XPL from sample 7.3.3, where it can be seen that the calcite mineral shows 2nd order twinning.

lattice preferred orientation. The sample containing organic material in the form of graphite together with mica's, monazite, pyrite, rutile, calcite, k-feldspar, zircon and quartz (see figure 25a and 25b). The mica's deformed ductile, whereas the k-feldspar deformed brittle. The quartz in this sample shows signs of dynamic recrystallization.

In sample 11.1, from the Northern limb of the Devonian rocks in Llavorsi-syncline near Burg (location 38), we see zircon, quartz, multiple mica's, apatite, calcite and pyrite. This pyrite again shows fringes on both sides parallel to the foliation. The thin-section shows a continuous S1 foliation, which has been intensively crenulated into an almost homogenous kink-band structure (*see figure 26*).
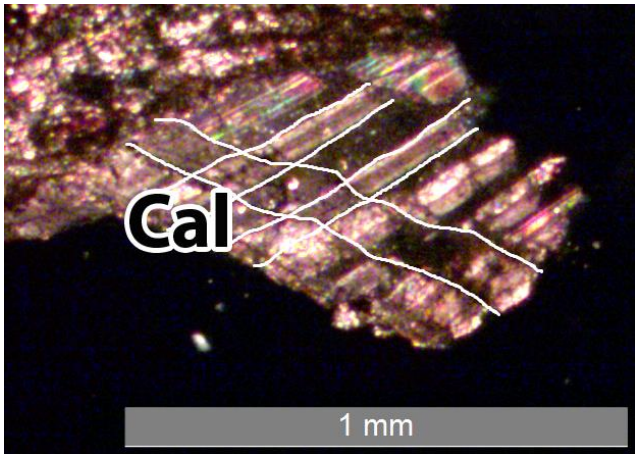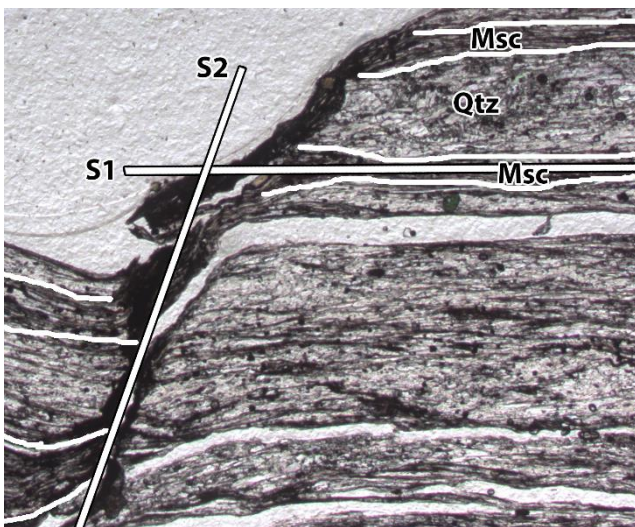

Figure 23, an image in PPL of Devonian rocks taken from the shear-bands near Llavorsi (location 33, sample 8.5). It shows the spaced S1 foliation, which is mainly built up of muscovite minerals, whereas the remainder is mainly quartz, chlorite and calcite. The shear-band (S2) cross-cut the S1 foliation. The original orientation of S2 is sub-horizontal and the displacement is top south.
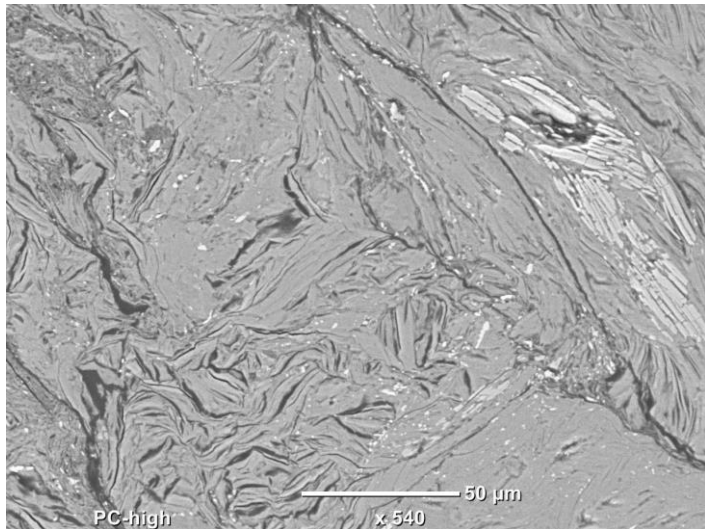
Figure 24, showing an image of sample 10.8.2 made by a scanning electron microscope, revealing the microscopic deformation of the Silurian black shales.
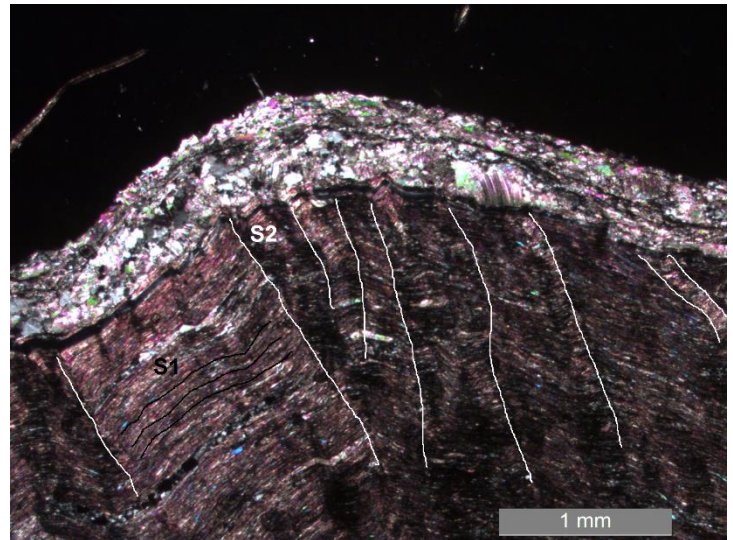

Figure 27, Showing a XPL image of sample 11.1 The black lines show the major penetrative foliation, and the white lines indicate the crenulation planes
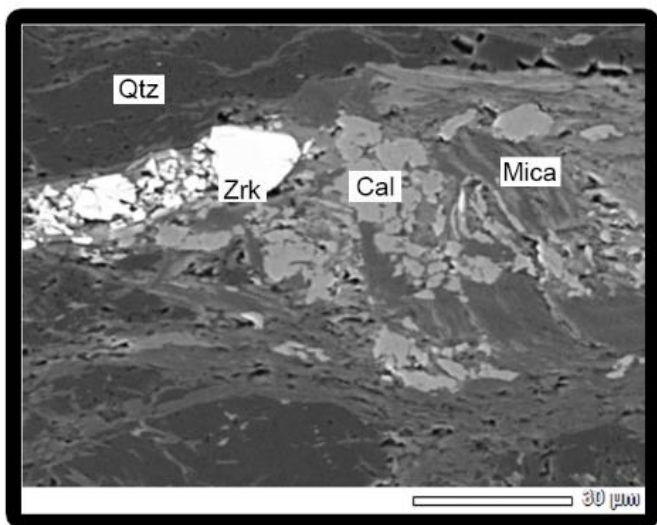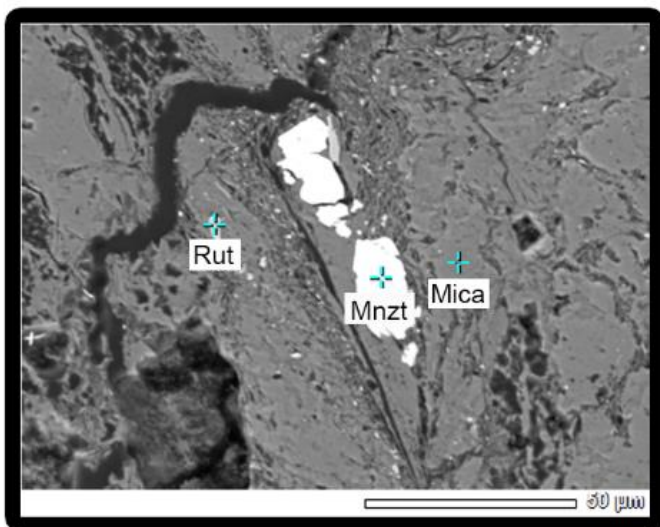

Figure 25a (above) and 25b (below) showing SEM images from sample 10.8.2, indicating its mineral composition. In this sample also monazite has been found (Mnzt).

6. Discussion

6.1 Kinematics

Regarding the results of the kinematic analysis, it can be seen that two dominant deformation phases have occurred in the Central Pyrenees with a third one, which occurred in between the two major phases. For D1, we find evidence that this deformation phase is of Variscan age because of the age of the rocks in which we find these structures. D1 resulted in the main foliation phase in the area (previously referred to as S1). This foliation can only be found in Paleozoic rocks up to the Upper Carboniferous. This would imply that the S1 foliation, and therefore also the general structure of the Llavorsi-syncline is of Variscan age, since we do not find these structures in Mesozoic rocks. In the Devonian rocks, we also find multiple shear zones, which show similar orientations to the foliations, which suggest an origin during the same event. This is confirmed by the fact that the larger faults in the Llavorsi area, on the northern and southern limb of the Llavorsi-syncline, show cross-cutting relations with the Maladeta-granite, which shows their Variscan age (*Muñoz, 1992*). In the Devonian rocks near Llavorsi, the shear- and kink-bands were also found. Due to the orientation of the crenulation of the foliation within the shear-bands of the Devonian near Llavorsi, it can be seen that there is a different deformation phase subsequent to the D1, which resulted in this S2 foliation (*see figure 12*). We call this the D2 deformation phase. It is likely that these kink- and shear-bands are formed during this D2. The Paleozoic rocks which encountered the D1 phase

	type I	type II	type III	type IV
Geometry **Description**	- thin twins - straight - rational - 1, 2 or 3 sets per grain	- thick (>>1μm) - straight - slightly lense shaped - rational	- curved thick twins - twins in twins - completely twinned - irrational	- thick, patchy - sutured twin boundaries - trails of tiny grains - irrational
Interpretations	- little deformation - little cover - very low temperature - (post-metamorphic) - (late tectonic)	- considerable deformation - completely twinned grains are possible - syn- or post-metamorphic deformation	- large deformation -intracrystalline deformation mechanisms (r-& f-glide) - syn-metamorphic deformation.	- large deformation - dynamic recrystallization (grain boundary migration) - pre- or syn-metamorphic deformation
Temperature	< 200°C	150-300°C	> 200°C	>250°C

Figure 27, A diagram showing the different types of twinning in calcite minerals (*Burkhard, 1993*)

underwent a second deformation phase D2, but it is unclear when this took place. In order to determine the age of the D2, the age of the muscovite minerals in the shear-bands can be determined. When we compare the Llavorsi-area, where these structures are clearly found, to the Port del Canto region, where we find the Mesozoic rocks, we can see a clear difference in orientation and direction of movement of the faults and shear zones. The structures in de Port del Canto region must be of Alpine age, due to the Permo-Triassic age of the rocks. This means these structures are caused by a post D1 deformation phase, namely the D3 deformation phase in the Central Pyrenees.

The PT conditions during D1 were different than during D3, this is reflected by the lack of ductile structures during D3. Therefore, D1 is largely responsible for the large infrastructure of the Axial Zone, whereas some of these structures are reactivated by the D3 phase. This can be concluded because of the scatter which can be seen in the orientations of the striations and stretching lineations. The large scatter of the D1 lineations compared to the narrow bandwidth of the direction of movement of the D3 structures suggests refolding or reactivation of older (D1) structures.

The kink-bands and shear-bands found in the Llavorsi area are younger than the S1, since they cross-cut and crenulate the structure (*see figure 14a and 14b*). The flat lying shear-bands in the Devonian strata near Llavorsi show a top south movement, which relates to shortening. The kink-bands in the same rocks also show a top south shear sense (see figure 12, 14a and 14b). The relative age between the kink-bands and shear-bands however is hard to determine, since these structures itself do not cross-cut. The shear-bands

are confined to weaker layers and run parallel to the S1 foliation in discrete zones of 5cm width. The kink-bands cross-cut the S1 foliation as well, but they do not cross-cut the shear-bands. This makes relative age determination very hard. When figure 12 is studied, it can be seen that the orientation of the kink-bands in the Devonian in the Llavorsi area (location 33) has a similar orientation but dips to the south. The similarity in orientation would suggest that these structures were formed as a conjugate set to faults within the Devonian rocks.

In the Vall de Boi the effects of the Alpine orogeny are also distinctively visible. As can be seen in figure 13, the S0 of both the Carboniferous and Devonian rocks dip to the NE, whereas the S1 foliation runs relatively flat throughout the rocks. Further South in the Vall de Boi, we find slightly overturned, very steep Triassic rocks. The rotation of the Triassic rocks is due to the Alpine orogeny, so if we assume the unconformable contact between the Carboniferous and the Triassic as a paleo-horizontal surface before the Alpine orogeny, the structures in the Carboniferous and Devonian rotate with it into a position where the S1 foliation becomes a steep structure. This reveals the S1 to be, just as in the Llavorsi area, the axial plane foliation of the folded Carboniferous and Devonian rocks (*see figure 28*) a structure of Variscan age.

The Alpine orogeny is also visible in the Vall d'Aran. The mylonite zone at the base of the Maladeta-granite shows ductile behavior and even shearing in the granodiorite itself (see figure 15b). The brittle deformed K-feldspar and dynamic recrystallized quartz indicate PT-conditions which happened after the formation of the Maladeta-granite, due to their low temperatures (~200°C - 300°C). This deformation also has had its effect on

Devonian hornfels in the Vall d' Aran where small shear zones were formed in between hornfels-boudins (*see figure 16*).

In the Llavorsi area, the Llavorsi-syncline itself has a tectonic contact on both the Northern and the southern limb. These faults are confined to a thin sequence of very incompetent Silurian black slates. These rocks accommodate all of the movement of the Northern and Southern fault. From the orientation of these faults, we can argue that these faults have been active during the Variscan orogeny, but when looking at at the direction of movement along the fault plane, which both on the southern limb as on the northern limb dip 50 degrees to the north and show N-S movement, it is likely that the fault has been reactivated during the Alpine orogeny, because kinematic indicators such as slickensides on the fault plane in the Silurian in the Southern limb of the Llavorsi syncline shows a top south shear-sense

whereas the fault in the Silurian in the northern limb shows a top north shear-sense. This difference could be caused by a later reactivation, since along the fault we find Cambro-Ordovician rocks on top of the Silurian and Devonian, meaning that there first must have been a top south orientation or tight folding leading to overturning of the northern limb. This can be seen in figure 18.3.

Thus, we can state that D1 consist of a compressional event during the Variscan orogeny which caused the main infrastructure of the Axial Zone in the Central Pyrenees. This deformation phase is characterized by a major foliation (S1) which runs ESE-WNW and dips around 50 degrees to the North together with major faults having a similar orientation. Direction of movement along these faults is in the NNE-SSW direction with considerable scatter of the plunging directions of the striations. At the end of the Variscan orogeny,
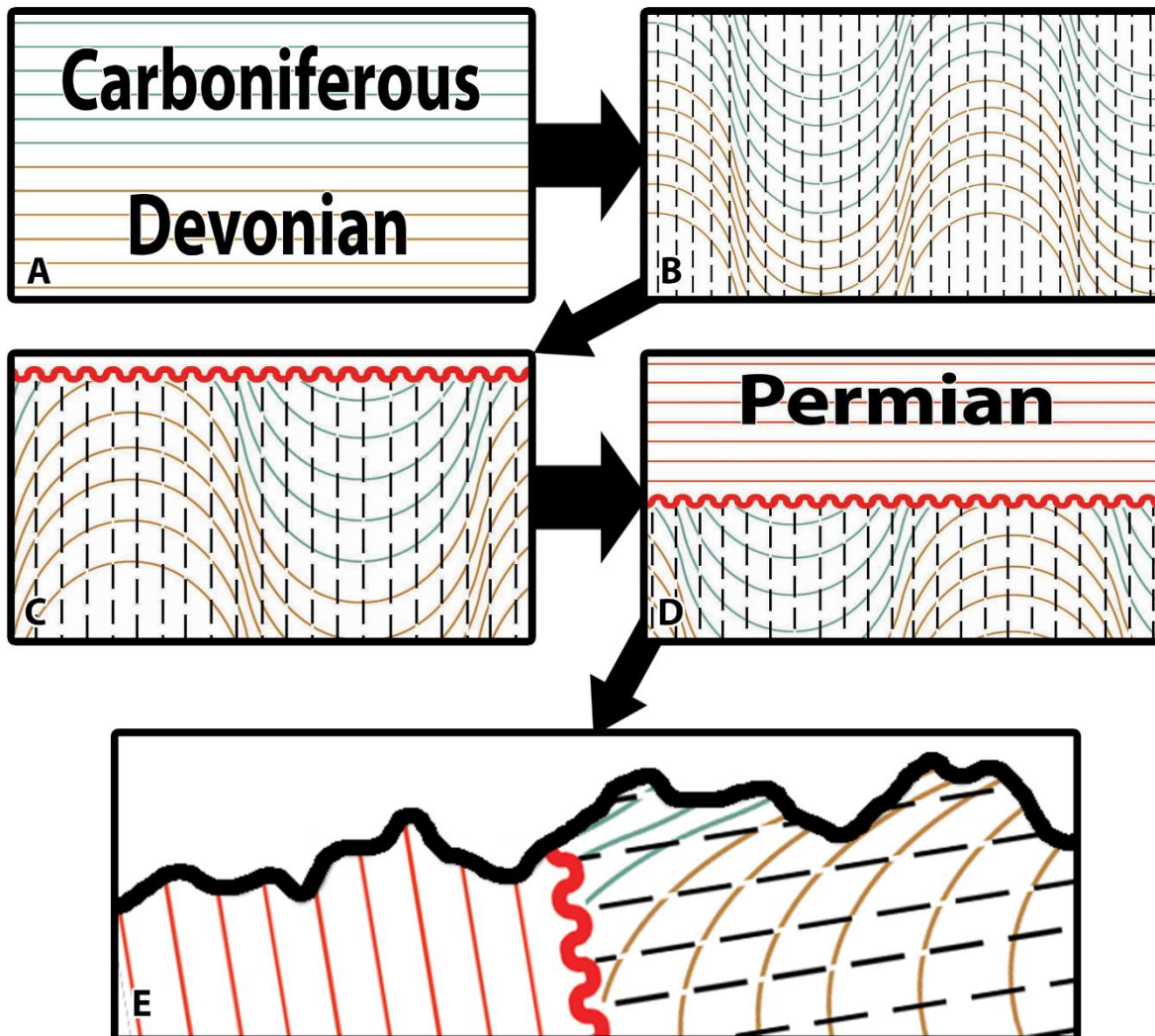

Figure 28, a schematic diagram of the tectonic evolution in the Vall de Boi region. After deposition of the Devonian and Carboniferous strata (A), the rocks were isoclinally folded by the Variscan Orogeny resulting in a widespread axial plane foliation (S1) (B). After the orogeny, the rocks eroded away, resulting in an erosional surface paleo-relief of Devonian and Carboniferous rocks (C). On this paleo-relief, Permian sandstones were deposited, unconformably overlying the Paleozoic rocks (D). During the Alpine orogeny, the rocks were rotated during the formation of the current Pyrenees and erosion of the area resulted in the present day topography in the area (E).

Figure 30, A diagram showing the relation between temperature and the geometry of the twins in calcite. The black dots resemble measurements from the studied thin sections in this study (*after Ferril, 2001*).
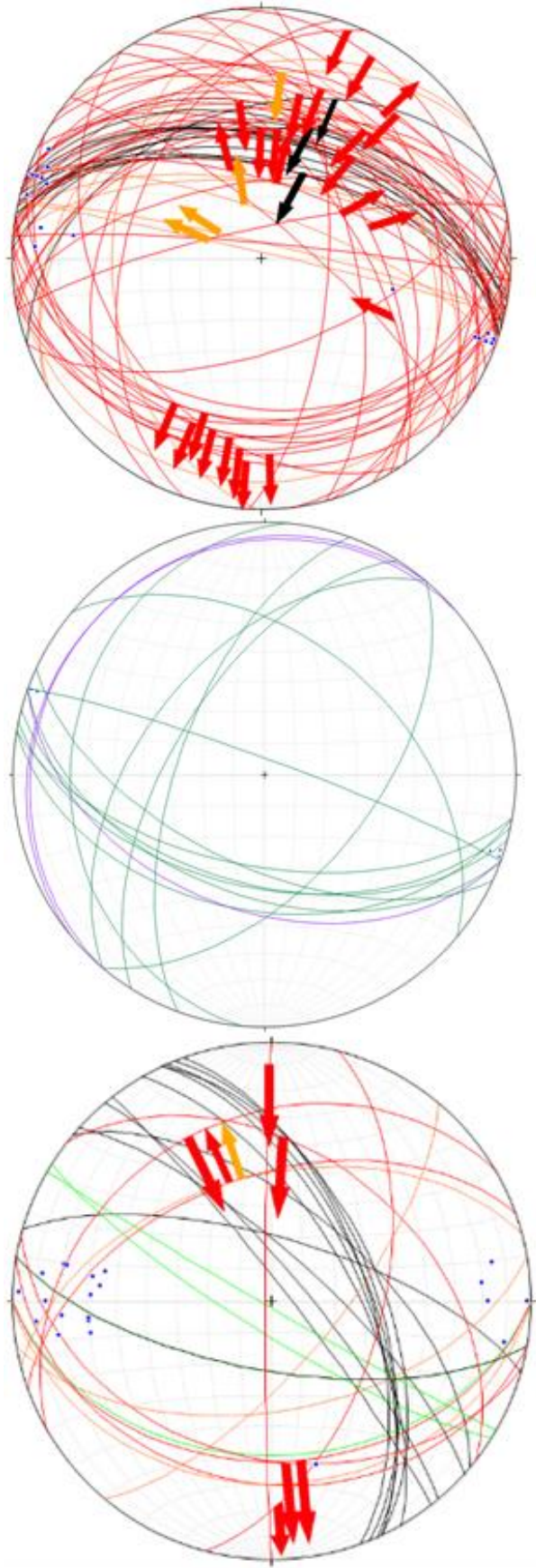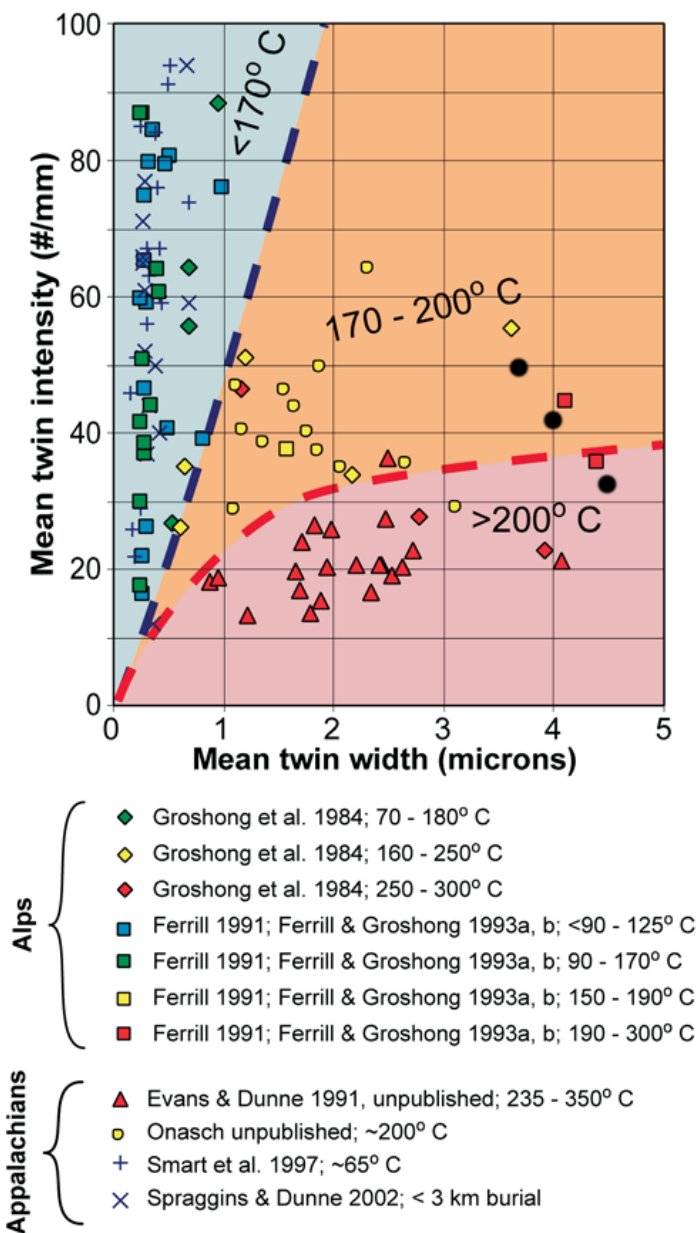
Figure 29a (above), 29b (middle) and 28c (below) showing combined stereographic projection of the D1, D2 and D3 structures in the field area respectively. Green great circles resemble kink-bands and purple great circles resemble shear-bands. The red great circles resemble faults with the red arrows indicating the striations. The green great circles in 28c resemble the unconformity between the Paleozoic rocks and the Permo-Triassic rocks. The black lines resemble the overturned Permo-Triassic S0 of the Vall de Boi.

around 300 Ma, the Maladeta-granite formed. This occurred during a time of extension in the Pyrenees (*Vissers, 1992*). The extension is explained by slab detachment underneath the Variscan Pyrenees (*Vissers, 2016*), which caused gravitational collapse and allowed the formation of the igneous bodies, such as for example the Maladeta (*Vissers, pers. comm.*). This intrusion resulted in contact-metamorphism in the surrounding rocks, turning them into hornfels.

During D2, a flat lying crenulation foliation (S2) of the S1 structures was formed in certain distinct bands in Paleozoic rocks (see figure 14a) During

the Alpine orogeny, which we can consider D3, a second compressional deformation phase
took place. During this deformation phase, the Paleozoic rocks formed, as a block, the Axial Zone of the current Pyrenees whereby certain Variscan faults, notably both of the faults on either side of the limbs of the Llavorsi-syncline, have been reactivated and others have formed. These newly formed faults show an E-W trend which show a direction of movement which is more N-S than D1. The scale of these structures can be in the order of kilometers. These D3 faults created the antiformal stack of the Axial Zone in the current Pyrenees. Some faults have a N-S to NNE-SSW strike, but these show major strike slip components in the same direction as the other faults. D3 has probably reactivated some of the D1 structures. This would explain the larger spread of orientations of the D1 structures in the stereographic projection, shown in figure 17.

6.2 Petrology
From the mineral composition of the studied samples it can be seen that the general composition of the rocks consist of quartz and mica, together with rutile, apatite, chlorite, calcite, zircon, monazite and pyrite. The studied thin-sections revealed deformed minerals showing dynamic recrystallization, lattice preferred orientations and twinning. By analyzing the twinning patterns in the calcite, it is possible to estimate the pressure and temperature conditions during deformation, since the type of calcite twin depends on the intensity of deformation (*Burkhard, 1993; Ferill, 2004*). The types of calcite twinning found in the calcite-bearing samples are type I and II twins, following the scheme in figure 27 (*Burkhard, 1993*). Plotting the measurements of the calcite twins observed in the thin sections in figure 30 gives a rough estimate of the temperature conditions during deformation of these calcite minerals, which lies around 200°C. The twinning of the calcite minerals happened during the Variscan Orogeny, this can be concluded from the fact that, as can be seen in figure 17.2, the S1 foliation and pressure solution seems parallel to the S1 wraps around the calcite minerals, making the minerals pre S1 and therefore deformation occurred during the Variscan orogeny. Using a geothermal gradient for the Axial-Zone of the Pyrenees during the Variscan orogeny of 50°C/km at the time of peak metamorphism (*García-Sansegundo, 1996*), we can estimate the depth of the around the time of deformation of the rocks currently exposed around Llavorsi to be 4 km. This results in an in situ lithostatic pressure of 107 Mpa. The dynamic recrystallization of quartz

and the brittle behavior of K-feldspar in sample 7.3.1 and 7.3.3 from the bottom of the Maladeta-granite however show temperature conditions of around 300°C. This deformation is of Alpine age, because Maladeta material is caught up in the shear zone, proving its post-Variscan activity. This is shown in the thin-sections taken from the base of the base of the Maladeta-granite, at the contact with the Devonian hornfels (location 2; figure 15).

7. Conclusion

From this research it can be concluded that there is a slight difference in the Axial Zone of the Pyrenees between the kinematics of the Variscan (D1) and Alpine (D3) orogeny. The shortening direction in the Alpine orogeny was N-S, whereas the shortening direction of the Variscan orogeny shows a small deviation, in the order of a few degrees, to the NNE-SSW. The major foliation in the studied area, the S1 foliation, is an axial plane foliation of the major structure in the Llavorsi-syncline. Both the formation of the Llavorsi-syncline itself and the S1 foliation are of Variscan age. The absolute age of the S2 foliation is unclear. Stereonet projections of the D1, D2 and D3 structures can be found in figures 29a, 29b and 29c. The Alpine orogeny may have reactivated some of the Variscan structures, resulting in a larger spread of the striations indicating direction of movement along Variscan structures. During the Alpine orogeny the large faults, the Nogueres- and Llavorsi-fault, were formed which resulted in the antiformal stack of the current axial zone.

Analysis of the sampled rocks revealed that the main composition of the meta-sediments in the Axial Zone consists of quartz and mica-minerals. Additional mineral assemblages consist of pyrite, calcite with traces of zircon, monazite and apatite. In the Silurian rocks, there was also organic material in the form of graphite present. From the analysis of the twinning in calcite minerals, we can conclude that the pressure and temperature conditions of the rocks during deformation lie around the 107 Mpa and 300°C. This deformation took place during the Variscan Orogeny. During Alpine orogeny, the temperature conditions were more around 350°C, as is proven by the dynamic recrystallization of quartz and the brittle behavior of K-feldspar in the mylonite zone at the base of the Maladeta. This, together with the found mineral assemblages would confirm that the region around Llavorsi resembles green schist facies metamorphism. A summary of the chain of events can be found in figure 31 below.
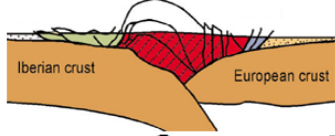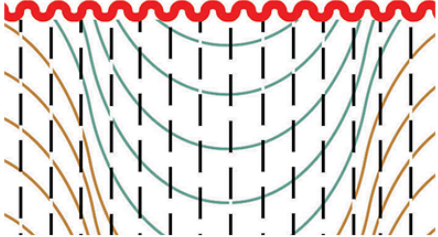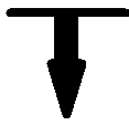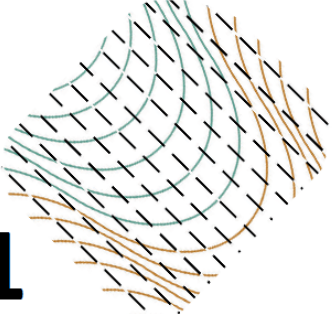
Time	Tectonic event	Deformation event
Present **Ceno-zoic**		D3 Antiformal stacking
	Alpine orogeny	Inversion
-100 Ma-	↑	
Meso-zoic		Erosion
-200 Ma-	**Rifting**	
		D2 Crenulation cleavage
Paleo-zoic	**Intrusions** ↓	
-300 Ma-		
	Variscan orogeny	**D1**
-400 Ma-	↑	**Axial plane foliation**
450 Ma		

Figure 31, showing a schematic summary of the deformation history of the Axial Zone of the Pyrenees near Llavorsi. After the Variscan orogeny, where a penetrative S1 axial plane foliation had developed throughout the region which dipped around 50 degrees to the north, the Maladeta intrusion was implaced during a period of extension due to gravitational collapse. Around this time, the S2 and C' structures were formed. Eventually, the current geometry of the Pyrenees was created by inversion due to the Alpine orogeny and the antiformal stacks of the central Pyrenees was created.

23

8. Acknowledgements

9. References

Boschma, D., 1963; *Successive Hercynian structures in some areas of the Central Pyrenees,* Leidse Geologische Mededelingen, vol. 28, pp. 103-176

Burkhard, M., 1993; *Calcite twins, their geometry, appearance and significance as stress-strain markers and indicators of tectonic regime: a review,* Journal of Structural Geology, vol. 15, pp. 351-368

Choukroune, P., 1989; *The ECORS Pyrenean deep seismic profile reflection data and the overall structure of an orogenic belt,* Tectonics, Vol. 8, pp. 23-39

Choukroune, P., Roure, F., Pinet, B., 1990; *Main results of the ECORS Pyrenees profile,* Tectonophysics, vol. 173, pp. 411-418

Choukroune, P., 1992; *Tectonic evolution of the Pyrenees,* Annual review of Earth and planetary sciences, vol. 20, pp. 143-158

Cocherie, A., Baudin, T., Aultran, A., Guerrot, C., Fanning, C.M., Laumonier, B., 2005; *U-Pb zircon (ID-TIMS and SHRIMP) evidence for the early Ordovician intrusion of metagranites in the Late Proterozoic Canaveilles Group of the Pyrenees and the Montagne Noir (France),* Bulletin de la Societe Geologique de France, vol. 176, pp. 269-282

Daignieres, M., Gallart, J., Banda, E., Hirn, A., 1982; *Implications for the seismic structure for the orogenic evolution of the Pyrenean Range,* Earth and Planetary Science Letters, vol. 57, pp. 88-100

Denele, Y., Pierre, B., Etienne, D., Ewan, P., Philippe, O.A., Gérard, G., 2009; *Middle Ordovician U-Pb age of the Aston and Hospitalet orthogneissic laccoliths: Their role in the Variscan evolution of the Pyrenees.* Bulletin de la Societe Geologique de France, vol. 180, pp. 209-216

Evans, N.G., Gleizes, G., LeBlanc, D., Bouchez, J.L., 1998; *Syntectonic emplacement of the Maladeta granite (Pyrenees) deduced from relationships between Hercynian deformation and contact metamorphism,* Journal of the Geological Society, vol. 155, pp. 209-216

Fitzgerald, P.G., Muñoz, J.A., Coney, P.J., Baldwin, S.L., 1999; *Asymmetric exhumation across the Pyrenean orogen: Implications for the tectonic evolution of a collisional orogen.* Earth and Planetary Science Letters, vol. 173, pp. 157-170

Ferril, D.A., Morris, A.P., Evans, M.A., Burkhard, M., Groshong jr., R.H., Onasch, C.M., 2004; *Calcite twin morphology: a low-temperature deformation geothermometer,* Journal of Structural Geology, vol. 26, pp. 1521-1529

Filleaudeau, P.Y., Mouthereau, F., Pik, R., 2012; *Thermo-tectonic evolution of the south-central Pyrenees from rifting to orogeny: insights from detrital zircon U/Pb and (U-Th)/He thermochronology,* Basin Research, vol. 23, pp. 1-17

García-Sansegundo, J., 1996; *Hercynian structure of the Axial Zone of the Pyrenees: the Aran Valley cross-section (Spain-France),* Journal of Structural Geology, vol. 18, pp. 1215-1325

Harteveld, J.J.A., 1970; *Geology of the upper Segre and Valira Valleys, Central Pyrenees, Andorra/Spain,* Leidse Geologische Mededelingen, vol. 45, pp. 167-236

Lagabrielle, Y., Labaume, P., Saint Blanquat, M. de,, 2010; *Mantle exhumation, crustal denudation, and gravity tectonics during Cretaceous rifting in the Pyrenean realm (SW Europe): Insights from the geological setting of the Iherzolite bodies,* Tectonics, vol. 29

Lapré, J.F., 1965; *Minor structures in the Upper Vicdessos Valley (Aston Massif, France),* Leidse Geologische Mededelingen, vol. 33, pp. 255-274

Losantos, M., Palau, J., Sanz, J., 1986; *Considerations about Hercynian thrusting in the Marimanya massif (Central Pyrenees),* Tectonophysics, vol. 129, pp. 71-79

Majeste-Menjoulas, C., 1979; *Evolution Alpine d'un segment de chaînes Varisque: Nappe de Gavarnie – Chevauchement Cinq-Monts Gentiane.* Travaux du Laboratoire de Geologie-Petrologie et du Laboratoire de Geologie Mediterraneene et Pyreneenne Associe au C.N.R.S., These Doctorale de Universite Paul Sabatier Toulouse

Martinius, A.W., 2012; *Contrasting styles of siliciclastic tidal deposits in a developing thrust-sheet-top basins – The Lower Eocene of the Central Pyrenees (Spain),* Principals of tidal sedimentology, Springer, chapter 18, pp. 473-506

Matte P., 2001; *The Variscan collage and orogeny (480-290 Ma) and the tectonic definition of the Armorica microplate: A review,* Terra Nova, vol. 13, pp. 122-128

McCaig, A.M., Wickham, S.M., 1984; *The tectonic evolution of the Pyrenees: A workshop,* Journal of the Geological Society, vol. 141, pp. 379-381

Metcalf, J.R., Fitzgerald, P.G., Baldwin, S.L., Muñoz, J.A., 2009; *Thermochronology of a convergent orogen: Constraints on the timing of thrust faulting and subsequent exhumation of the Maladeta Pluton in the Central Pyrenean Axial Zone,* Earth and Planetary Science Letters, vol. 287, pp. 488-503

Mey, P.H.W., 1967; *The geology of the upper Ribagorzana and Baliera Valleys, Central Pyrenees, Spain,* Leidse Geologische Mededelingen, vol. 41, pp. 153-220

Mey, P.H.W., 1968; *Geology of the upper Ribagorzana and Tor Valleys, Central Pyrenees, Spain,* Leidse Geologische Mededelingen, vol. 41, pp. 229-292

Muller, J., Roger, P., 1977; *L'evolution des Pyrénées (domaine central et occidental), Le segment Hercynien, la chaine de fond Alpine,* Geologie Alpine, vol. 53, pp. 141-191

Muñoz, J.A., 1992; *Evolution of a continental collision belt: ECORS-Pyrenees crustal balanced cross-section,* in Thrust Tectonics by McClay, pp. 235-246

Oele, J.A., 1966; *The stuctural history of the Vall Ferrera Area, the transition zone between the Aston Massif and the Salat-Pallaresa anticlinorium (Central Pyrenees, France, Spain),* Leidse Geologische Mededelingen, vol. 38, pp. 129-164

Olivet, J.L, 1996; *Kinematics of the Iberian plate,* Bulletin des Centres de Recherches Elf Exploration Production, vol. 20, pp. 191-195

Le Pichon, X., Sibuet, J.C., 1971; *Western extension of boundary between European and Iberian plates during the Pyrenean Orogeny,* Earth and Planetary Science Letters, vol. 12, pp. 83-88

Rahl, J.M., Haines, S.H., van der Pluijm, B.A., 2011; *Links between orogenic wedg deformation and erosional exhumation: Evidence from illite age analysis of fault rock and detrital thermochronology of syntectonic conglomerates in the Spanish Pyrenees,* Earth and Planetary Science Letters, vol. 307, pp. 180-190

Roest, W.R., Srivastava, S.P., 1991; *Kinematics of the plate boundaries between Eurasia, Iberia and Africa in the North Atlantic from the Late Cretaceous to the present,* Geology, vol. 19, pp. 613-616

Seguret, M., 1970; *Étude tectonique des nappes et series décollées de la partie central du versant sud des Pyrénées.* PhD thesis, Montpellier

Sibuet, J.C., Srivastava, S.P., Spakman, W., 2004; *Pyrenean orogeny and plate kinematics¸* Journal of Geophysical Research, vol. 109

Verges, J., Millán, H., Roca, E., Muñoz, J.A., Marzo, M., Cirés, J., Den Bezemer, T., Zoetemeijer, R., Cloetingh, S., 1995; *Eastern Pyrenees and related foreland basins: Pre-, syn- and post-collisional crustal-scale cross-sections,* Marine and Petroleum Geology, vol. 12, pp. 893-915

Vissers, R.L.M., 1992; *Variscan extension in the Pyrenees,* Tectonics, vol. 11, pp. 1369-1384

Vissers, R.L.M., Meijer, P.T., 2012; *Iberian plate kinematics and Alpine collision in the Pyrenees,* Earth-Science Reviews, vol. 114, pp. 61-83

Vissers, R.L.M., Hinsbergen, D.J.J. van, Meer, D.G. van der, Spakman, W., 2016; *Cretaceous slab break-off in the Pyrenees: Iberian plate kinematics in paleomagnetic and mantle reference frames*, Gondwana Research, vol. 34, pp. 49-59

Zandvliet, J., 1960; *The geology of the upper Salat and Pallaresa Valleys, Central Pyrenees, France/Spain,* Leidse Geologische Mededelingen, vol. 25, pp. 1-127

Zwart, H.J., 1954; *La géologie du massif du Saint-Barthélémy, Pyrénées, France,* Leidse Geologische Mededelingen, vol. 18, pp. 1-228

Zwart, H.J., 1959; *Metamorphic history of the Central Pyrenees, part 1*, Leidse Geologische Mededelingen, vol. 22, pp. 419-490

Zwart, H.J., 1979; *Leidse Geologische Mededelingen deel 50*.

Zwart, H.J., 1986; *The Variscan geology of the Pyrenees,* Tectonophysics, vol. 129, pp. 9-27